Wave Field Synthesis with Primary Source Correction: Theory, Simulation Results, and Comparison to Earlier Approaches

Florian Völk and Hugo Fastl

AG Technische Akustik, MMK, Technische Universität München, Arcisstraße 21, 80333 München, Germany

Correspondence should be addressed to Florian Völk (`florian.voelk@mytum.de`)

ABSTRACT
Wave-field synthesis (WFS) with primary-source correction (PSC) extends earlier theoretical derivations by the correct synthesis of primary point sources at a reference point. In this paper, the theory of WFS with PSC is revised with respect to other derivations, extended for the application to focus points, and validated by numerical simulation. A comparison to earlier approaches to WFS concludes the paper.

1. INTRODUCTION

Wave-field synthesis (WFS) for audio applications has been introduced in the late 1980's by the group around A. J. Berkhout at Delft University of Technology, the Netherlands (Berkhout 1988, Berkhout and de Vries 1989). WFS aims at synthesizing physically correct a reference sound pressure field, the primary field, within a specified spatial region, the listening area or volume (Berkhout et al. 1993).

Theoretically, WFS is possible within a listening volume, based on the Kirchhoff-Helmholtz integral equation (KHI), employing an infinite number of secondary monopole and dipole point sources distributed contin-uously on the listening volume boundary area (three-dimensional WFS, Vogel 1993). Simple primary fields are spherical, cylindrical, and plane waves, while the synthesis of more complex wave fields is feasible, too (Boone et al. 1995). Based on the KHI, different mathematical derivations of WFS have been given (Berkhout 1988, Berkhout et al. 1993, Vogel 1993, Verheijen 1997, Spors 2005, Spors et al. 2008).

In typical implementations, the number of secondary sources is reduced by degenerating the boundary area to a boundary contour, and therefore the three-dimensional (3D) scenario to a two-dimensional (2D). Further, the integration over the closed boundary area

(3D) or contour (2D) can be degenerated to integration over an infinitely extended plane or line (Williams 1999). In all 2D situations, it would be necessary to replace the secondary point sources by secondary line sources with parallel axes along a specific coordinate direction. The procedure is then referred to as 2D WFS (Verheijen 1997). To allow for 2D WFS, the primary field must be independent of one coordinate direction (Williams 1999), preventing the simulation of fully three-dimensional as for example spherical fields. This restriction is disregarded by some authors, resulting in erroneous synthesized fields (e. g. Spors 2005, Spors et al. 2008).

The theoretically infinitely extended secondary line sources are typically realized by single point sources (2.5D WFS), requiring a correction term in the derivation, referred to as stationary phase approximation (Berkhout et al. 1993, Start 1997, Verheijen 1997) or secondary source correction (Spors 2005, Spors et al. 2008). The major consequence of secondary point instead of line sources is that the synthesized field is correct at a reference point only for closed boundary contours (Start 1996) or on a reference line parallel to a linear secondary source distribution (de Vries 1996). Earlier secondary source corrections are based on far-field and high-frequency approximations, often disregarding phase relations (Start 1997, Spors et al. 2008), resulting in erroneous fields, especially in the near-field and low-frequency regions. Most WFS systems are realized using monopole secondary sources only (Verheijen 1997, Spors et al. 2008), requiring further adaption of the theory, which is possible only approximately and causes further synthesis errors (Spors 2007a,b).

Since it is impossible to realize continuous source distributions, discretized secondary source arrays are employed, resulting in aliasing artifacts in the generated field in the frequency range above the spatial aliasing frequency (Corteel 2006, Wittek et al. 2007, Corteel et al. 2008, Spors and Ahrens 2009).

In this paper, the derivation of WFS is revised for continuous secondary source distributions, primarily based on Spors et al. (2008), resulting in a thorough and well defined theoretical framework, including a general formulation of the secondary source correction that reduces the synthesis error over the whole listening area and allows for a correct amplitude and phase reproduction at the reference point. Furthermore, the

primary-source correction (PSC) introduced by Völk et al. (2011) is discussed and extended to focus points, permitting the correct synthesis of spherical waves evolving at arbitrary distances in the plane defined by the listening area. 2D and 2.5D WFS with PSC result in the correct inverse proportionality of level and distance for primary point sources at the correct absolute level, which is shown not to hold true for previous approaches of simulating primary spherical waves by means of WFS.

The paper is structured as follows: Initially, continuous 3D WFS is discussed, followed by simple primary source models for WFS, including refinements of the current literature. On that basis, the derivations of 2D and 2.5D WFS are revised, resulting in a general formulation of primary and secondary source correction, allowing for the correct reproduction of spherical waves. Finally, with regard to the implementation of WFS, monopole only WFS is discussed, based on the theoretical framework introduced here, and compared to previous approaches.

2. LISTENING VOLUME: THREE-DIMENSIONAL (3D) WAVE FIELD SYNTHESIS

In this paper, time dependent variables are denoted by lower case letters, for example the sound pressure at the position $\mathbf{x}$ in an arbitrary coordinate system is represented by $p(\mathbf{x}) = p(\mathbf{x}, t)$, while frequency dependent variables are indicated by upper case letters, e. g. $P(\mathbf{x}) = P(\mathbf{x}, \omega)$. The explicit notation of the time and frequency dependences is omitted for convenience where not explicitly required.

According to Williams (1999, equation 8.15), the KHI can be written to describe the homogeneous acoustic pressure field $p(\mathbf{x})$ within the source-free listening volume V, while no field exists outside V (interior KHI). Being $P(\mathbf{x})$ the temporal Fourier transform of $p(\mathbf{x})$,

$$\frac{\partial}{\partial \mathbf{n}} P(\mathbf{x}_0) = \langle \nabla P(\mathbf{x}), \mathbf{n}(\mathbf{x}_0) \rangle \big|_{\mathbf{x}=\mathbf{x}_0} \qquad (1)$$

represents the directional gradient of the sound pressure spectrum $P(\mathbf{x}_0)$ on the volume surface S_0 (Bronstein et al. 2001, equation 13.34, p. 670). Here, $\mathbf{x}_0 \in S_0$ holds and $\mathbf{n}(\mathbf{x}_0)$ denotes the inward normal to the surface S_0 at $\mathbf{x}_0$. The inward normal is typically used in WFS (Verheijen 1997, Spors et al. 2008), while the outward normal is employed by Williams

This paper was presented at the 133$^{\text{rd}}$ Convention of the Audio Engineering Society 2012, as paper number 8717.

Page 2 of 20

(1999). Therefore the sign is inverted compared to Williams' definition here (cf. also Skudrzyk 1971, equation 20, p. 492). On that basis, the KHI describes the pressure field

$$P(\mathbf{x}) = - \oiint_{S_0} \left[G_{3D}(\mathbf{x}|\mathbf{x}_0) \frac{\partial}{\partial \mathbf{n}} P(\mathbf{x}_0) - \right.$$
$$\left. - P(\mathbf{x}_0) \frac{\partial}{\partial \mathbf{n}} G_{3D}(\mathbf{x}|\mathbf{x}_0) \right] dS_0, \quad (2)$$
$$\forall \mathbf{x} \in V, \ \mathbf{x} \notin S_0, \ \mathbf{x}_0 \in S_0$$

dependent on the pressure spectrum $P(\mathbf{x}_0)$ and its directional gradient $\frac{\partial}{\partial \mathbf{n}} P(\mathbf{x}_0)$ on S_0. Here,

$$G_{3D}(\mathbf{x}|\mathbf{x}_0) = \frac{\mathrm{e}^{-\mathrm{j}k|\mathbf{x}-\mathbf{x}_0|}}{4\pi |\mathbf{x}-\mathbf{x}_0|}, \qquad \forall \mathbf{x} \neq \mathbf{x}_0 \quad (3)$$

represents the 3D free field Green's function (Skudrzyk 1971, equation 29, p. 645), a solution of the inhomogeneous wave equation for excitation with a spatio-temporal Dirac impulse at $\mathbf{x}_0$ (Spors et al. 2008, p. 2). In other words, $G_{3D}(\mathbf{x}|\mathbf{x}_0)$ describes the spatio-temporal transfer characteristics of the path from a monopole point source at $\mathbf{x}_0$ to $\mathbf{x} \neq \mathbf{x}_0$.

$$k = \frac{\omega}{c} = \frac{2\pi f}{c} = \frac{2\pi}{\lambda} \quad (4)$$

represents the acoustical wave number, with the temporal frequency f, the speed of sound c, and the wave lengt λh (Zollner and Zwicker 1993). The directional gradient

$$\frac{\partial}{\partial \mathbf{n}} G_{3D}(\mathbf{x}|\mathbf{x}_0) = \left(\frac{1}{|\mathbf{x}-\mathbf{x}_0|} + \mathrm{j}k \right) \times$$
$$\times \frac{(\mathbf{x}-\mathbf{x}_0)^{\mathrm{T}} \mathbf{n}(\mathbf{x}_0)}{|\mathbf{x}-\mathbf{x}_0|} G_{3D}(\mathbf{x}|\mathbf{x}_0), \quad \forall \mathbf{x} \neq \mathbf{x}_0 \quad (5)$$

of the 3D free space Green's function in boundary normal direction $\mathbf{n}(\mathbf{x}_0)$ represents the spatio-temporal transfer characteristics of a dipole point source at $\mathbf{x}_0$, with its main axis in direction $\mathbf{n}(\mathbf{x}_0)$ and evaluated at $\mathbf{x} \neq \mathbf{x}_0$ (Spors et al. 2008, p. 2/3). Note that the directional gradient must be taken with respect to $\mathbf{x}_0$ here (Pierce 1998, p. 165/166, in contrast to Spors 2005, equation 2.66).

In the context of WFS, the KHI is interpreted in that the pressure field within the source free listening volume V can be controlled by an appropriately driven secondary source distribution on the volume surface S_0. The secondary source characteristics are described by the free space 3D Green's function (monopole point source) and its directional gradient (dipole point source), while the driving functions, the spectra of the signals driving the secondary sources, are given by the primary sound pressure spectrum and its directional gradient on S_0. Speaking descriptively, a continuous distribution of monopole and dipole secondary sound sources along S_0 allows to fully control the pressure field inside the source free listening volume V bounded by S_0, where no field arises outside V. To synthesize a specific primary field, each monopole secondary source must be driven by the directional gradient of the primary pressure field at the respective secondary source position $\mathbf{x}_0$ along the inward normal $\mathbf{n}(\mathbf{x}_0)$ on S_0, while the dipole sources are driven by the primary pressure at $\mathbf{x}_0$ (3D WFS). It is possible to degenerate the listening volume to a half space, limited by an infinitely extended plane and a half-sphere of infinite radius. The integration is then reduced to the infinitely extended plane (Spors et al. 2008, p. 7).

3. PRIMARY SOURCE MODELS

The primary sound field to be generated by WFS must be given by its sound pressure spectrum $P(\mathbf{x}_0)$ on the volume boundary S_0 with $\mathbf{x}_0 \in S_0$ and the corresponding directional gradient in direction of the inward normal $\mathbf{n}(\mathbf{x}_0)$ on S_0 (cf. equation 2). Consequently, arbitrary source free sound fields can be synthesized within V if the sound pressure distribution and its directional gradient on S_0 are known. This knowledge may be acquired either by measurement (data-based) or analytically, based on primary source models (model-based, Vorländer 2008). Typically applied simple primary source models are plane, spherical, and cylindrical wave fields (Spors et al. 2008, p. 5). More complex primary source models for WFS have been developed by Warufsel et al. (2004), Baalman (2005, 2007), Ahrens and Spors (2007), and Corteel (2007).

Using the sound pressure spectrum $\hat{P}_{\mathrm{a}}$ on a sphere or cylinder with radius $a \to 0$ around a primary monopole point or line source according to Zollner and Zwicker (1993, equations 2.91 and 2.110), simple primary source models are formulated in the following. For the models being primary source models for WFS, the field variable is without loss of generality denoted $\mathbf{x}_0 \in S_0$ here. Each model is given

This paper was presented at the 133rd Convention of the Audio Engineering Society 2012, as paper number 8717.

Page 3 of 20

in form of a primary pressure field $P_{\mathrm{pf}}(\mathbf{x}_0)$, the corresponding directional gradient $\frac{\partial}{\partial \mathbf{n}}P_{\mathrm{pf}}(\mathbf{x}_0)$, and the local propagation direction $\mathbf{n}_{\mathrm{pf}}(\mathbf{x}_0)$ at $\mathbf{x}_0$.

3.1. Plane Waves
Plane sound waves (PWs) can be regarded as created by an infinite plane, oscillating in normal direction $\mathbf{n}_{\mathrm{pw}}$. In that case, areas of equal pressure are planes and the sound field is independent of two coordinate directions of each Cartesian coordinate system with the remaining axis in field normal direction (Zollner and Zwicker 1993, section 2.2). The independence of two Cartesian coordinate directions is indicated here by the upper index *1D*, for example $\mathbf{x}^{\mathrm{1D}}$.

According to Skudrzyk (1971, equation 5, p. 313), the spectrum of a plane propagating sound pressure field is given by

$$\begin{aligned} P_{\mathrm{pw}}(\mathbf{x}_0) &= \mathrm{e}^{-\mathrm{j}k\mathbf{n}_{\mathrm{pw}}^{\mathrm{T}}\mathbf{x}_0}\hat{P}_{\mathrm{a}} \\ &= \mathrm{e}^{-\mathrm{j}k\mathbf{n}_{\mathrm{pw}}^{\mathrm{1D,T}}\mathbf{x}_0^{\mathrm{1D}}}\hat{P}_{\mathrm{a}} = P_{\mathrm{pw}}(\mathbf{x}_0^{\mathrm{1D}}). \end{aligned} \tag{6}$$

The corresponding gradient in normal direction $\mathbf{n}(\mathbf{x}_0)$ can be described with equation 1 by

$$\begin{aligned} \frac{\partial}{\partial \mathbf{n}}P_{\mathrm{pw}}(\mathbf{x}_0) &= k\,\mathrm{e}^{-\mathrm{j}\frac{\pi}{2}}\mathbf{n}_{\mathrm{pw}}^{\mathrm{T}}\mathbf{n}(\mathbf{x}_0)P_{\mathrm{pw}}(\mathbf{x}_0) \\ &= k\,\mathrm{e}^{-\mathrm{j}\frac{\pi}{2}}\mathbf{n}_{\mathrm{pw}}^{\mathrm{1D,T}}\mathbf{n}(\mathbf{x}_0^{\mathrm{1D}})P_{\mathrm{pw}}(\mathbf{x}_0^{\mathrm{1D}}) \\ &= \frac{\partial}{\partial \mathbf{n}}P_{\mathrm{pw}}(\mathbf{x}_0^{\mathrm{1D}}). \end{aligned} \tag{7}$$

3.2. Spherical Waves
Spherical sound waves (SWs) are radiated concentrically from a point source at $\mathbf{x}_{\mathrm{p}}$. Then, the sound pressure on spherical shells is constant (Zollner and Zwicker 1993, section 2.3).

Skudrzyk (1971, equation 23, p. 349) gives the spectrum of spherical sound pressure fields by

$$P_{\mathrm{sw}}(\mathbf{x}_0|\mathbf{x}_{\mathrm{p}}) = \frac{\mathrm{e}^{-\mathrm{j}k|\mathbf{x}_0-\mathbf{x}_{\mathrm{p}}|}}{|\mathbf{x}_0-\mathbf{x}_{\mathrm{p}}|}\hat{P}_{\mathrm{a}}, \quad \forall \mathbf{x}_0 \neq \mathbf{x}_{\mathrm{p}}. \tag{8}$$

If the spherical wave is employed as a primary source model for WFS, $\mathbf{x}_{\mathrm{p}} \notin V$ holds, for the KHI being valid exclusively for source free volumes. With the local propagation direction of the pressure field

$$\mathbf{n}_{\mathrm{sw}}(\mathbf{x}_0) = \frac{\mathbf{x}_0-\mathbf{x}_{\mathrm{p}}}{|\mathbf{x}_0-\mathbf{x}_{\mathrm{p}}|}, \quad \forall \mathbf{x}_0 \neq \mathbf{x}_{\mathrm{p}} \tag{9}$$

and equation 1, the directional gradient of the field spectrum in direction $\mathbf{n}(\mathbf{x}_0)$ is given by

$$\begin{aligned} \frac{\partial}{\partial \mathbf{n}}P_{\mathrm{sw}}(\mathbf{x}_0|\mathbf{x}_{\mathrm{p}}) &= \left(\frac{1}{|\mathbf{x}_0-\mathbf{x}_{\mathrm{p}}|}+\mathrm{j}k\right)\mathrm{e}^{\mathrm{j}\pi}\times \\ &\times \mathbf{n}_{\mathrm{sw}}^{\mathrm{T}}(\mathbf{x}_0)\mathbf{n}(\mathbf{x}_0)P_{\mathrm{sw}}(\mathbf{x}_0|\mathbf{x}_{\mathrm{p}}), \quad \forall \mathbf{x}_0 \neq \mathbf{x}_{\mathrm{p}}. \end{aligned} \tag{10}$$

3.3. Cylindrical Waves
Concentrically diverging cylindrical waves (CWs) are radiated from an infinitely extended pulsating cylinder, a line source. The field is symmetric with regard to the cylinder axis, and areas of constant pressure are cylinder shells (Zollner and Zwicker 1993, section 2.5). Furthermore, the field is independent of the coordinate direction parallel to the cylinder axis. In the paper on hand, the independence of one coordinate direction is indicated by the upper index *2D*, for example $\mathbf{x}_0^{\mathrm{2D}}$.

According to Skudrzyk (1971, equations 34 and 36, p. 427), the pressure field spectrum of a line source located at $\mathbf{x}_{\mathrm{p}}^{\mathrm{2D}}$ is given by

$$\begin{aligned} P_{\mathrm{cw}}(\mathbf{x}_0^{\mathrm{2D}}|\mathbf{x}_{\mathrm{p}}^{\mathrm{2D}}) &= H_0^{(2)}\left(k\left|\mathbf{x}_0^{\mathrm{2D}}-\mathbf{x}_{\mathrm{p}}^{\mathrm{2D}}\right|\right)\hat{P}_{\mathrm{a}}\times \\ &\times \pi\,\mathrm{e}^{-\mathrm{j}\frac{\pi}{2}}, \quad \forall\left(k\left|\mathbf{x}_0^{\mathrm{2D}}-\mathbf{x}_{\mathrm{p}}^{\mathrm{2D}}\right|\right)>0. \end{aligned} \tag{11}$$

Note the deviation by the factor $-\pi/4$ to the cylindrical pressure field spectrum given by Spors (2005, equation 2.40). Here, $H_0^{(2)}(x)$ denotes the Hankel function of the second kind, zeroth order. According to Abramowitz and Stegun (1972, equations 9.1.3 and 9.1.4), the Hankel functions of the first and second kinds, nth order are defined by

$$H_{\mathrm{n}}^{(1)}(x) = J_{\mathrm{n}}(x) + \mathrm{j}Y_{\mathrm{n}}(x) \quad \text{and} \tag{12}$$

$$H_{\mathrm{n}}^{(2)}(x) = J_{\mathrm{n}}(x) - \mathrm{j}Y_{\mathrm{n}}(x), \ \forall x > 0, \ n \in \mathbb{Z}_0^+, \tag{13}$$

with the Bessel functions of the first and second kinds $J_{\mathrm{n}}(x)$ and $Y_{\mathrm{n}}(x)$ (cf. Bronstein et al. 2001, p. 527). For large arguments, the Hankel functions may according to Bronstein et al. (2001, equation 9.56a and 9.56c, p. 529) be approximated by

$$H_{\mathrm{n}}^{(1)}(x) \approx \sqrt{\frac{2}{\pi x}}\,\mathrm{e}^{\mathrm{j}\left(x-n\frac{\pi}{2}-\frac{\pi}{4}\right)} \quad \text{and} \tag{14}$$

$$\begin{aligned} H_{\mathrm{n}}^{(2)}(x) &\approx \sqrt{\frac{2}{\pi x}}\,\mathrm{e}^{-\mathrm{j}\left(x-n\frac{\pi}{2}-\frac{\pi}{4}\right)}, \\ &\quad \forall x \gg 1, \ n \in \mathbb{Z}_0^+. \end{aligned} \tag{15}$$

This paper was presented at the 133$^{\mathrm{rd}}$ Convention of the Audio Engineering Society 2012, as paper number 8717.

Page 4 of 20

Combining the local propagation direction of a cylindrical pressure field

$$\mathbf{n}_{cw}(\mathbf{x}_0^{2D}) = \frac{\mathbf{x}_0^{2D} - \mathbf{x}_p^{2D}}{\left|\mathbf{x}_0^{2D} - \mathbf{x}_p^{2D}\right|}, \qquad \forall \mathbf{x}_0^{2D} \neq \mathbf{x}_p^{2D}, \quad (16)$$

the Hankel functions of the first and second kinds, zeroth order (equations 12 and 13), and

$$\frac{\partial}{\partial \mathbf{n}} H_0^{(2)}(k|\mathbf{x}|) = -kH_1^{(2)}(k|\mathbf{x}|)\frac{\mathbf{x}^T \mathbf{n}}{|\mathbf{x}|}, \quad (17)$$
$$\forall (k|\mathbf{x}|) > 0$$

(computed with equation 1 in combination with Zollner and Zwicker 1993, equation 2.74), the sound pressure gradient spectrum of a line source located at $\mathbf{x}_p^{2D}$ in normal direction $\mathbf{n}(\mathbf{x}_0^{2D})$ at $\mathbf{x}_0^{2D}$ is given by

$$\frac{\partial}{\partial \mathbf{n}} P_{cw}(\mathbf{x}_0^{2D}|\mathbf{x}_p^{2D}) = H_1^{(2)}\left(k\left|\mathbf{x}_0^{2D} - \mathbf{x}_p^{2D}\right|\right) \times$$
$$\times \hat{P}_a k\pi\, e^{j\frac{\pi}{2}} \mathbf{n}_{cw}^T(\mathbf{x}_0^{2D})\mathbf{n}(\mathbf{x}_0^{2D}), \quad (18)$$
$$\forall \left(k\left|\mathbf{x}_0^{2D} - \mathbf{x}_p^{2D}\right|\right) > 0.$$

3.4. Focus Points

The KHI in its representation employed here is based on a source free listening volume V (cf. section 2). For that reason, it is not possible to synthesize primary sources within V by WFS. However, a hypothetic and idealized wave field may converge in one half-space to a focus point $\mathbf{x}_p$ or focus line $\mathbf{x}_p^{2D}$ located in V and diverge in the other half-space, while equaling zero on the half-space dividing plane except the focus point $\mathbf{x}_p$ or focus line $\mathbf{x}_p^{2D}$ (Lucas and Muir 1982). In other words, this field resembles the field of an acoustic sink in one half space, but the field of an acoustic source in the other. Such a field can be regarded as emerging from a source distribution outside V, and can for that reason be generated by WFS, approximating the field of a source within V in the subspace with the diverging field. Consequently, approximately valid synthesis results are possible only in the subspace with the diverging field. In the context of WFS, the focus points or lines are usually referred to as focused sources (Boone et al. 1996, Verheijen 1997, Wittek et al. 2004).

Errors in the diverging field are introduced by the discontinuity of the hypothetic field discussed here at the half-space dividing plane. To reduce errors

resulting from discontinuities, truncation windows can be applied (Start 1997, section 4.2). For the simulations in this paper, squared cosine windows with the only zeros at the dividing plane are used.

The half-spaces are distinguished here based on the half-space dividing plane normal in direction of the diverging field, referred to as $\mathbf{n}_{fs}(\mathbf{x}_{ref,fs}|\mathbf{x}_p)$ for focus points and $\mathbf{n}_{fs}(\mathbf{x}_{ref,fs}^{2D}|\mathbf{x}_p^{2D})$ for focus lines. These normals are given at the focus point or line with respect to a reference point $\mathbf{x}_{ref,fs}$ or line $\mathbf{x}_{ref,fs}^{2D}$ in the subspace with the diverging field by

$$\mathbf{n}_{fs}(\mathbf{x}_{ref,fs}|\mathbf{x}_p) = \frac{\mathbf{x}_{ref,fs} - \mathbf{x}_p}{|\mathbf{x}_{ref,fs} - \mathbf{x}_p|}. \quad (19)$$

Pressure and directional pressure gradient at the secondary source contour S_0 in the half-space with the diverging field are given by the field of a spherical or line source at $\mathbf{x}_p$ or $\mathbf{x}_p^{2D}$ (Verheijen 1997, section 2.3.2). In the half-space with the field converging towards the focus point or line, the pressure and directional pressure gradient can be derived from the fields of point and line sources using the so-called time-reversal principle (Jackson and Dowling 1991, Fink 1992, Fink and Prada 2001, Yon et al. 2003a): the sound pressure transmissions from the secondary sources to the focus point or line can be regarded as time and phase inverted transmissions from a point respectively line source at the focus point or line to the secondary sources (Tanter et al. 2001, Kim et al. 2001, Yon et al. 2003b). In other words: the pressure field converging to the focus point or line and its directional gradient are time and phase inverted versions of the pressure field and gradient of a point respectively line source at the focus point.

For generating a synchronous and causal overall system, a pre-delay must be applied to allow for the time-reversal (Ahrens and Spors 2008). A spherical wave radiated from $\mathbf{x}_p$ at $t = t_0 = 0\,\text{s}$ reaches the secondary source position $\mathbf{x}_0$ at

$$t = t_1(\mathbf{x}_0|\mathbf{x}_p) = t_0 + \frac{|\mathbf{x}_0 - \mathbf{x}_p|}{c} = \frac{|\mathbf{x}_0 - \mathbf{x}_p|}{c}. \quad (20)$$

If the time is inverted with respect to $t_0 = 0\,\text{s}$, that is if t is substituted by $-t$, the wave front is radiated at $t = -t_1(\mathbf{x}_0|\mathbf{x}_p)$ and reaches the focus point or line at $t = t_0 = 0\,\text{s}$. If a causal system is to be designed, a pre-delay

$$\Delta t_{fs} \geq t_1(\mathbf{x}_0|\mathbf{x}_p) = \frac{|\mathbf{x}_0 - \mathbf{x}_p|}{c} \quad (21)$$

This paper was presented at the 133rd Convention of the Audio Engineering Society 2012, as paper number 8717.

Page 5 of 20

has to be applied to the overall system. Because it is typically desired not to introduce unnecessary delay, the minimum delay $\Delta t_{\mathrm{fs_{min}}}$ resulting in a causal system is usually selected, given using the maximum distance between a secondary source and the focus point respectively focus line $\max\left(|\mathbf{x}_0 - \mathbf{x}_{\mathrm{p}}|\right)$ by

$$\Delta t_{\mathrm{fs_{min}}} = \frac{\max\left(|\mathbf{x}_0 - \mathbf{x}_{\mathrm{p}}|\right)}{c}. \tag{22}$$

If a synchronous and causal overall system is to be derived, the pre-delay must be applied to non-focused sources, too. Let $p(t)$ represent the sound pressure at a fixed position, which is a real-valued time function created by a real and stable system. Then, the corresponding Fourier transform $P(\omega)$ is Hermitian and

$$P(-\omega) = P^*(\omega) \tag{23}$$

holds (Oppenheim et al. 1998, equation 4.30). According to the Fourier transform similarity theorem (Marko 1995, equation 4.3), a time reversal is reflected spectrally by the frequency reversal

$$p(-t) \circ\!\!-\!\!\bullet \ P(-\omega) = P^*(\omega). \tag{24}$$

Using equations 22 and 24 and the Fourier transform time shifting property (Oppenheim et al. 1998, equation 4.27), the frequency domain representation of a time inverted sound pressure time function temporally shifted by $\Delta t_{\mathrm{fs_{min}}}$ is given by

$$p\left(-t - \Delta t_{\mathrm{fs_{min}}}\right) \circ\!\!-\!\!\bullet \ P^*(\omega)\, \mathrm{e}^{-\mathrm{j}\omega\Delta t_{\mathrm{fs_{min}}}}. \tag{25}$$

While the focusing procedure is given exemplary here for a focus point, an analogous derivation holds for the focus line. Using equations 8, 9, 19, 25, combined with the phase inversion, the pressure field of a focus point at $\mathbf{x}_{\mathrm{p}} \in V$ is given by

$$P_{\mathrm{fsw}}(\mathbf{x}_0|\mathbf{x}_{\mathrm{p}}) =$$
$$= \begin{cases} P_{\mathrm{sw}}(\mathbf{x}_0|\mathbf{x}_{\mathrm{p}})\, \mathrm{e}^{-\mathrm{j}k\max(|\mathbf{x}_0 - \mathbf{x}_{\mathrm{p}}|)} \\ \quad \text{if } \langle \mathbf{n}_{\mathrm{sw}}(\mathbf{x}_0), \mathbf{n}_{\mathrm{fs}}(\mathbf{x}_{\mathrm{ref,fs}}|\mathbf{x}_{\mathrm{p}})\rangle > 0, \\ P_{\mathrm{sw}}^*(\mathbf{x}_0|\mathbf{x}_{\mathrm{p}})\, \mathrm{e}^{-\mathrm{j}[k\max(|\mathbf{x}_0 - \mathbf{x}_{\mathrm{p}}|)-\pi]} \\ \quad \text{if } \langle \mathbf{n}_{\mathrm{sw}}(\mathbf{x}_0), \mathbf{n}_{\mathrm{fs}}(\mathbf{x}_{\mathrm{ref,fs}}|\mathbf{x}_{\mathrm{p}})\rangle < 0, \\ 0 \quad \text{otherwise.} \end{cases} \tag{26}$$

The corresponding directional gradient of a focus point in secondary source contour normal direction

$\mathbf{n}(\mathbf{x}_0)$ is given with equations 10, 9, 19, 25, combined with the phase inversion by

$$\frac{\partial}{\partial\mathbf{n}}P_{\mathrm{fsw}}(\mathbf{x}_0|\mathbf{x}_{\mathrm{p}}) =$$
$$= \begin{cases} \dfrac{\partial}{\partial\mathbf{n}}P_{\mathrm{sw}}(\mathbf{x}_0|\mathbf{x}_{\mathrm{p}})\, \mathrm{e}^{-\mathrm{j}k\max(|\mathbf{x}_0 - \mathbf{x}_{\mathrm{p}}|)} \\ \quad \text{if } \langle \mathbf{n}_{\mathrm{sw}}(\mathbf{x}_0), \mathbf{n}_{\mathrm{fs}}(\mathbf{x}_{\mathrm{ref,fs}}|\mathbf{x}_{\mathrm{p}})\rangle > 0, \\ \dfrac{\partial}{\partial\mathbf{n}}P_{\mathrm{sw}}^*(\mathbf{x}_0|\mathbf{x}_{\mathrm{p}})\, \mathrm{e}^{-\mathrm{j}[k\max(|\mathbf{x}_0 - \mathbf{x}_{\mathrm{p}}|)-\pi]} \\ \quad \text{if } \langle \mathbf{n}_{\mathrm{sw}}(\mathbf{x}_0), \mathbf{n}_{\mathrm{fs}}(\mathbf{x}_{\mathrm{ref,fs}}|\mathbf{x}_{\mathrm{p}})\rangle < 0, \\ 0 \quad \text{otherwise.} \end{cases} \tag{27}$$

4. LISTENING AREA: TWO-DIMENSIONAL (2D) WAVE FIELD SYNTHESIS

According to Williams (1999, p. 266), acoustic problems can be simplified assuming a 3D field to be constant along an arbitrary chosen coordinate direction. In the context of WFS, the resulting situation is typically referred to as 2D WFS, while the reproduction still takes place in the 3D space (Sonke et al. 1998, Sonke 2000, Spors et al. 2008). Following Williams (1999, p. 266), a conversion from the 3D KHI to a 2D problem is possible by neglecting geometrical dependencies along the dimension the situation is assumed constant, and replacing the 3D by the 2D free space Green's function

$$G_{\mathrm{2D}}(\mathbf{x}^{\mathrm{2D}}|\mathbf{x}_0^{\mathrm{2D}}) = \frac{\mathrm{e}^{-\mathrm{j}\frac{\pi}{2}}}{4}H_0^{(2)}\left(k\,|\mathbf{x}^{\mathrm{2D}} - \mathbf{x}_0^{\mathrm{2D}}|\right), \tag{28}$$
$$\forall \left(k\,|\mathbf{x}^{\mathrm{2D}} - \mathbf{x}_0^{\mathrm{2D}}|\right) > 0$$

(Skudrzyk 1971, equation 87, p. 656). Note the inverted sign compared to the definition given by Spors (2005, equation 2.68) respectively Spors et al. (2008, equation 22). The 2D free space Green's function may be regarded as the spatio-temporal transfer characteristics of a monopole line source located at $\mathbf{x}_0^{\mathrm{2D}}$, extended in the constant coordinate direction, and evaluated at $\mathbf{x}^{\mathrm{2D}}$ (Spors et al. 2008).

Using the Hankel function of the first kind, zeroth order (equation 12) and equation 17, the directional gradient of the 2D free space Green's function with respect to $\mathbf{x}_0^{\mathrm{2D}}$ is given by

$$\frac{\partial}{\partial\mathbf{n}}G_{\mathrm{2D}}(\mathbf{x}^{\mathrm{2D}}|\mathbf{x}_0^{\mathrm{2D}}) = H_1^{(2)}\left(k\,|\mathbf{x}^{\mathrm{2D}} - \mathbf{x}_0^{\mathrm{2D}}|\right) \times$$
$$\times\, k\frac{\mathrm{e}^{-\mathrm{j}\frac{\pi}{2}}}{4}\frac{(\mathbf{x}^{\mathrm{2D}} - \mathbf{x}_0^{\mathrm{2D}})^{\mathrm{T}}\mathbf{n}(\mathbf{x}_0^{\mathrm{2D}})}{|\mathbf{x}^{\mathrm{2D}} - \mathbf{x}_0^{\mathrm{2D}}|}, \tag{29}$$
$$\forall \left(k\,|\mathbf{x}^{\mathrm{2D}} - \mathbf{x}_0^{\mathrm{2D}}|\right) > 0.$$

This paper was presented at the 133rd Convention of the Audio Engineering Society 2012, as paper number 8717.

Page 6 of 20

The directional gradient of the 2D free space Green's function represents the spatio-temporal transfer characteristics of a dipole line source at $\mathbf{x}_0^{2D}$, extended along the constant coordinate direction, positioned with its main axis along $\mathbf{n}(\mathbf{x}_0^{2D})$, and evaluated at $\mathbf{x}^{2D} \in (A \setminus x_0)$.

With equations 28 and 29, the 3D KHI (equation 2) is adapted to a two-dimensional situation: within a source-free listening area A, the spectrum $P(\mathbf{x}^{2D})$ of the sound pressure field $p(\mathbf{x}^{2D})$ is given by the spectrum of the pressure distribution on the area boundary contour x_0 and its directional gradient in inward normal direction $\mathbf{n}(\mathbf{x}_0^{2D})$ with $\mathbf{x}_0^{2D} \in x_0$ by

$$P(\mathbf{x}^{2D}) = -\oint_{x_0} \left[G_{2D}(\mathbf{x}^{2D}|\mathbf{x}_0^{2D}) \frac{\partial}{\partial \mathbf{n}} P(\mathbf{x}_0^{2D}) - \right.$$
$$\left. - P(\mathbf{x}_0^{2D}) \frac{\partial}{\partial \mathbf{n}} G_{2D}(\mathbf{x}^{2D}|\mathbf{x}_0^{2D}) \right] dx_0, \quad (30)$$
$$\forall \mathbf{x}^{2D} \in A, \ \mathbf{x}^{2D} \notin x_0, \ \mathbf{x}_0^{2D} \in x_0, \ k > 0.$$

It is possible to interpret equation 30 in the context of WFS in that the pressure field within the listening area A, bounded by the contour x_0, and all parallel areas can be controlled by an appropriately driven secondary line source distribution perpendicular to A on x_0. The secondary source characteristics are given by the 2D free space Green's function (monopole line source) and its directional gradient (dipole line source). Here, appropriately driven means the monopole line sources driven by the directional gradient of the primary pressure field at the respective secondary source position in inward normal direction on x_0, while the dipole sources are driven by the primary pressure at their positions.

It is important to note that the primary field must not depend on the coordinate direction given by the axes of the secondary line sources (the 2D Green's functions). This fact restricts primary fields for 2D WFS to fields independent of the coordinate direction perpendicular to the listening area, which is with their normal at every field point in the listening area. Components with other propagation directions *cannot be synthesized correctly*, especially including primary spherical waves, regardless of their origin. Since the WFS derivation of Spors et al. (2008, equation 29) disregards this restriction, errors in the synthesized field show up (cf. also Spors 2005).

Errors are here defined as differences between synthesized and targeted fields; a positive level error for example indicates a synthesized field of higher level than the reference field.

Figure 1 shows the errors of 2D WFS according to equation 30 for spherical primary fields according to equations 8, 9, 10, 26, 27, and a circular secondary source contour of 1.3 m radius (indicated by the vertical dash-dotted gray line), centered at the origin $\mathbf{x}_a = [0\ 0\ 0]^T$ of a Cartesian coordinate system.
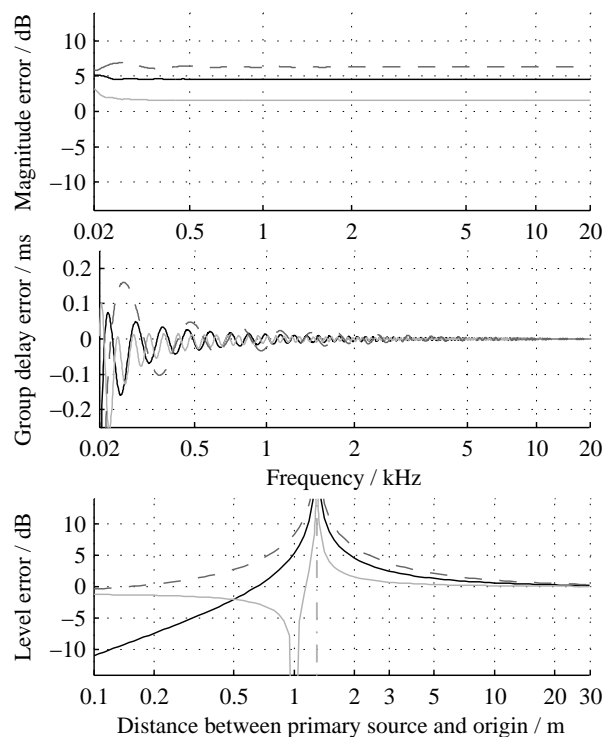
Fig. 1: Deviation of the pressure field created by 2D wave-field synthesis from the targeted spherical field at $\mathbf{x} = [0\ 0\ 0]^T$ (black), $\mathbf{x} = [1\ 0\ 0]^T$ (solid light gray), and $\mathbf{x} = [-1\ 0\ 0]^T$ (dashed dark gray), for a circular secondary source contour centered at $\mathbf{x}_a = [0\ 0\ 0]^T$ (radius 1.3 m, dash-dotted). The upper two panels show the frequency dependent magnitude and group delay errors of the spherical field originating at $\mathbf{x}_p = [2\ 0\ 0]^T$, the lower panel shows the average level error in the range $f = 1\ldots5$ kHz over the distance $|\mathbf{x}_p|$ between the origin and the variable primary source position.

Each panel holds data computed for three evaluation positions: the center of the secondary source contour

This paper was presented at the 133rd Convention of the Audio Engineering Society 2012, as paper number 8717.

Page 7 of 20

$(\mathbf{x} = [0\ 0\ 0]^{\mathrm{T}}$, black), a position closer to the source $(\mathbf{x} = [1\ 0\ 0]^{\mathrm{T}}$, solid light gray), and a position farther away from the source $(\mathbf{x} = [-1\ 0\ 0]^{\mathrm{T}}$, dashed dark gray). The evaluation positions are selected on the line defined by the field origin and the secondary source contour midpoint so that the magnitudes and characteristics of possible errors are reflected. The errors at evaluation positions shifted perpendicular to the line are comparable in their characteristics but of reduced magnitude. This geometric configuration is used throughout this paper to allow for comparisons of the scenarios.

The upper two panels show the frequency dependent magnitude and group delay errors. The magnitude errors are in the range of some 5 dB and rather frequency independent, varying by about ±3 dB within the secondary source contour. Level differences of more than 1 dB are audible (Fastl and Zwicker 2007, p. 180). An erroneous overall level in WFS most likely results in erroneous distance perception, considering the absolute level to be an important cue for the auditory distance perception (Zahorik et al. 2005). The group delay errors decrease with increasing frequency, with maximum values of some ±100 µs at frequencies in the range around 50 Hz. Regarding the temporal resolution, the human hearing system is most sensitive for interaural delays, which are an important cue for the directional hearing, with a just noticeable interaural delay in the range of 50 µs (Fastl and Zwicker 2007, p. 293). This being said, the group delay errors at low frequencies may be perceivable, especially on head movements, possibly resulting in erroneous directional hearing.

The lower panel shows exemplary the average level error in the frequency range between $f = 1\,\mathrm{kHz}$ and $f = 5\,\mathrm{kHz}$ for different distances $|\mathbf{x}_{\mathrm{p}}|$ between origin and primary source. Since the level error is rather frequency independent in that frequency range (cf. upper panel), the average is assumed a good indicator for the overall level error. The error exceeds 10 dB for primary sources close to the secondary source contour, and decays globally with the distance between primary source and secondary source contour. The distance perception is likely to be influenced by the level error, especially for primary source distances below 10 m, where the human distance perception shows its highest accuracy (Zahorik 2002, Zahorik et al. 2005, Völk 2010, Völk et al. 2012). The verti-

cal dash-dotted line indicates the radius of the secondary source contour and therefore the transition between point sources and focus points. The gray contour shows the error at the evaluation position $\mathbf{x} = [1\ 0\ 0]^{\mathrm{T}}$, located towards the primary source between the origin and the secondary source contour. Since focused sources are valid only in the sub-space with diverging waves, the gray contour must be interpreted carefully in the converging field, which is for distances $|\mathbf{x}_{\mathrm{p}}| < 1\,\mathrm{m}$.

The cause of the errors shown here is independent of the secondary source geometry, and comparable errors result for circular secondary source contours of different radius and for differently shaped closed secondary source contours. Summarizing, when using the approach of Spors (2005) respectively Spors et al. (2008) of simulating spherical waves by 2D WFS, deviations in level and group delay are likely to be audible, with level and group delay errors dependent on the primary source position.

5. PRIMARY SOURCE CORRECTION IN 2D WAVE FIELD SYNTHESIS

The sound fields radiated by all sources of dimensions small compared to the wavelength of the sound can be approximated for large distances by spherical fields (Zollner and Zwicker 1993, p. 75). This being said, the inability of 2D WFS to generate primary spherical waves means a severe restriction.

For that reason, 2D primary-source correction (PSC) according to Völk et al. (2011) is discussed and extended to focus points here. 2D PSC allows at a reference point $\mathbf{x}_{\mathrm{ref,psc}}^{\mathrm{A}}$ within the listening area A for the correct 2D WFS of primary point sources at $\mathbf{x}_{\mathrm{p}}^{\mathrm{A}}$ in the plane defined by the listening area.

Using equations 11, 18, and 30, the pressure field generated by 2D WFS of a primary line source at $\mathbf{x}_{\mathrm{p}}^{\mathrm{2D}} \notin (A \cup x_0)$ with the cylinder axis perpendicular to the listening area is described by its spectrum

$$
\begin{aligned}
P_{\mathrm{cw}}&(\mathbf{x}^{\mathrm{2D}}|\mathbf{x}_{\mathrm{p}}^{\mathrm{2D}}) = \\
&= -\oint_{x_0} \left[G_{\mathrm{2D}}(\mathbf{x}^{\mathrm{2D}}|\mathbf{x}_0^{\mathrm{2D}})\frac{\partial}{\partial \mathbf{n}}P_{\mathrm{cw}}(\mathbf{x}_0^{\mathrm{2D}}|\mathbf{x}_{\mathrm{p}}^{\mathrm{2D}}) - \right. \\
&\quad \left. - P_{\mathrm{cw}}(\mathbf{x}_0^{\mathrm{2D}}|\mathbf{x}_{\mathrm{p}}^{\mathrm{2D}})\frac{\partial}{\partial \mathbf{n}}G_{\mathrm{2D}}(\mathbf{x}^{\mathrm{2D}}|\mathbf{x}_0^{\mathrm{2D}}) \right]dx_0, \\
&\quad \forall\, \mathbf{x}^{\mathrm{2D}} \in (A \setminus x_0),\, \mathbf{x}_0^{\mathrm{2D}} \in x_0, \\
&\qquad \mathbf{x}_{\mathrm{p}}^{\mathrm{2D}} \notin (A \cup x_0),\, k > 0.
\end{aligned}
\tag{31}
$$

This paper was presented at the 133$^{\mathrm{rd}}$ Convention of the Audio Engineering Society 2012, as paper number 8717.

Page 8 of 20

It is possible without loss of generality to adjust the sound pressure in the field given by equation 31 at the reference point $\mathbf{x}_{\text{ref,psc}}^{\text{A}} \in (A \setminus x_0)$ to the pressure in the field of a primary point source at $\mathbf{x}_{\text{p}}^{\text{A}} = \left(\mathbf{x}_{\text{p}}^{\text{2D}} \cap A\right)$ by

$$P_{\text{sw}}(\mathbf{x}_{\text{ref,psc}}^{\text{A}}|\mathbf{x}_{\text{p}}^{\text{A}}) =$$
$$= P_{\text{cw}}(\mathbf{x}_{\text{ref,psc}}^{\text{A}}|\mathbf{x}_{\text{p}}^{\text{A}})\frac{P_{\text{sw}}(\mathbf{x}_{\text{ref,psc}}^{\text{A}}|\mathbf{x}_{\text{p}}^{\text{A}})}{P_{\text{cw}}(\mathbf{x}_{\text{ref,psc}}^{\text{A}}|\mathbf{x}_{\text{p}}^{\text{A}})} \quad (32)$$
$$= P_{\text{cw}}(\mathbf{x}_{\text{ref,psc}}^{\text{A}}|\mathbf{x}_{\text{p}}^{\text{A}})C_{\text{ps}}(\mathbf{x}_{\text{ref,psc}}^{\text{A}}|\mathbf{x}_{\text{p}}^{\text{A}}).$$

Here, the complex-valued, frequency dependent primary source correction factor

$$C_{\text{ps}}(\mathbf{x}_{\text{ref,psc}}^{\text{A}}|\mathbf{x}_{\text{p}}^{\text{A}}) = \frac{P_{\text{sw}}(\mathbf{x}_{\text{ref,psc}}^{\text{A}}|\mathbf{x}_{\text{p}}^{\text{A}})}{P_{\text{cw}}(\mathbf{x}_{\text{ref,psc}}^{\text{A}}|\mathbf{x}_{\text{p}}^{\text{A}})}$$
$$= \frac{\text{e}^{-\text{j}\left(k\left|\mathbf{x}_{\text{ref,psc}}^{\text{A}}-\mathbf{x}_{\text{p}}^{\text{A}}\right|-\frac{\pi}{2}\right)}}{\pi\left|\mathbf{x}_{\text{ref,psc}}^{\text{A}}-\mathbf{x}_{\text{p}}^{\text{A}}\right|H_0^{(2)}\left(k\left|\mathbf{x}_{\text{ref,psc}}^{\text{A}}-\mathbf{x}_{\text{p}}^{\text{A}}\right|\right)}, \quad (33)$$
$$\forall\left(k\left|\mathbf{x}_{\text{ref,psc}}^{\text{A}}-\mathbf{x}_{\text{p}}^{\text{A}}\right|\right) > 0$$

is derived using equations 8 and 11. Note that $C_{\text{ps}}(\mathbf{x}_{\text{ref,psc}}^{\text{A}}|\mathbf{x}_{\text{p}}^{\text{A}})$ is independent of the secondary source position $\mathbf{x}_0^{\text{2D}}$; the PSC is done with respect to the primary source position $\mathbf{x}_{\text{p}}^{\text{A}}$.

The field generated by 2D WFS with a primary cylindrical wave and PSC is given using equations 31 and 32 by

$$P_{\text{sw,psc,2D}}(\mathbf{x}^{\text{2D}}|\mathbf{x}_{\text{ref,psc}}^{\text{A}}|\mathbf{x}_{\text{p}}^{\text{A}}) =$$
$$= -\oint_{x_0}\left[G_{\text{2D}}(\mathbf{x}^{\text{2D}}|\mathbf{x}_0^{\text{2D}})\frac{\partial}{\partial\mathbf{n}}P_{\text{cw}}(\mathbf{x}_0^{\text{2D}}|\mathbf{x}_{\text{p}}^{\text{2D}})-\right.$$
$$\left.- P_{\text{cw}}(\mathbf{x}_0^{\text{2D}}|\mathbf{x}_{\text{p}}^{\text{2D}})\frac{\partial}{\partial\mathbf{n}}G_{\text{2D}}(\mathbf{x}^{\text{2D}}|\mathbf{x}_0^{\text{2D}})\right]dx_0 \times \quad (34)$$
$$\times C_{\text{ps}}(\mathbf{x}_{\text{ref,psc}}^{\text{A}}|\mathbf{x}_{\text{p}}^{\text{A}}),$$
$$\forall\mathbf{x}^{\text{2D}}, \mathbf{x}_{\text{ref,psc}}^{\text{A}} \in (A \setminus x_0), \mathbf{x}_0^{\text{2D}} \in x_0,$$
$$\mathbf{x}_{\text{p}}^{\text{2D}}, \mathbf{x}_{\text{p}}^{\text{A}} \notin (A \cup x_0), \ k > 0.$$

The result represents the field of a primary point source located in the plane defined by the listening area A exclusively at the reference point $\mathbf{x}_{\text{ref,psc}}^{\text{A}}$, while deviating from primary spherical and cylindrical fields at all other positions.

Figure 2 shows the deviation between the field of a point source at $\mathbf{x}_{\text{p}} = [2\ 0\ 0]^{\text{T}}$ approximated by

2D WFS with a primary cylindrical wave and PSC according to equation 34 with regard to the origin $(\mathbf{x}_{\text{ref,psc}}^{\text{A}} = [0\ 0\ 0]^{\text{T}})$ and the targeted spherical field for the configuration also shown by figure 1.
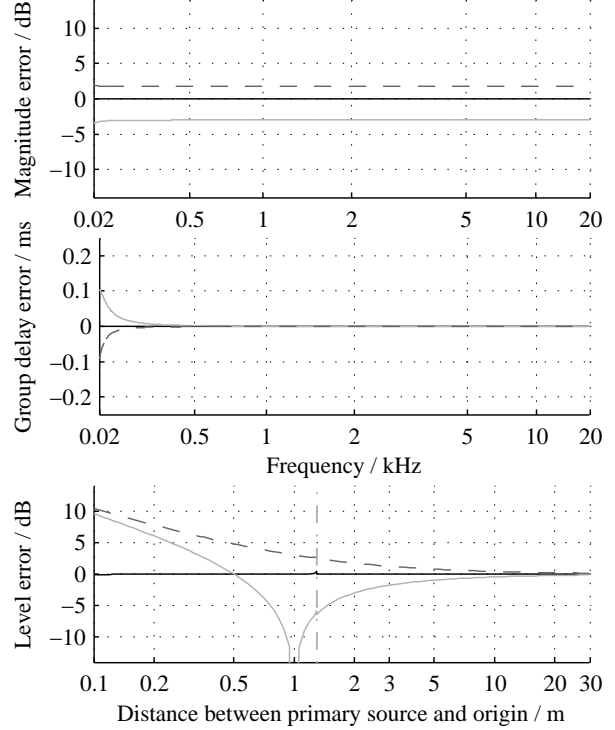
Fig. 2: Deviation of the pressure field created by 2D wave field synthesis with a cylindrical primary field and primary source correction (PSC) from the targeted spherical field. Geometry and evaluation positions identical to figure 1.

The synthesis is correct at the reference point, for all frequencies and primary source distances. The magnitude error at evaluation positions off the reference point proceeds approximately frequency independently in the range of $\pm 3\,\text{dB}$ (evaluation positions selected representative for the error range), showing slightly larger values in the direction of the primary source (solid light gray), compared to evaluation positions farther away than the reference point (dashed gray). Group delay errors in the range of $\pm 0.1\,\text{ms}$ occur at positions off the reference point at frequencies below $100\,\text{Hz}$.

The lower panel indicates the correct inverse proportionality of level and distance at the reference point.

This paper was presented at the 133$^{\text{rd}}$ Convention of the Audio Engineering Society 2012, as paper number 8717.

Page 9 of 20

For primary point sources (right from the dash-dotted horizontal line), deviations up to $5\,\mathrm{dB}$ occur for distances below some $10\,\mathrm{m}$ at evaluation points farther (dashed dark gray) and especially closer to the source than the reference point (solid light gray). Regarding focus points, the light gray curve is also shown for the erroneous field at distances between primary source and reference point below $1\,\mathrm{m}$. Apart from this invalid field, the level errors increase off the reference point up to some $10\,\mathrm{dB}$.

The reduction of the area of correct synthesis to a reference point means a severe restriction of 2D WFS with PSC, but allows at the reference point for the synthesis of primary point sources in the plane defined by the listening area. The PSC adds no restriction compared to primary spherical waves in 2D WFS, where the errors depend on the evaluation position, too (figure 1). As shown in the following section, WFS must be restricted to a reference point $\mathbf{x}_{\mathrm{ref,ssc}}^{\mathrm{A}}$ within the listening area if the secondary line sources are replaced by point sources in typical WFS implementations. If a common reference point for primary and secondary source correction $\mathbf{x}_{\mathrm{ref}}^{\mathrm{A}} = \mathbf{x}_{\mathrm{ref,psc}}^{\mathrm{A}} = \mathbf{x}_{\mathrm{ref,ssc}}^{\mathrm{A}}$ is selected, no additional restriction is imposed by PSC.

6. SECONDARY POINT SOURCES: 2.5D WAVE FIELD SYNTHESIS

Further reduction of complexity is typically achieved by replacing the secondary line sources in equation 30 by point sources located at $\mathbf{x}_0^{\mathrm{A}}$ in the listening area A, where $\mathbf{x}_0^{\mathrm{A}} = (\mathbf{x}_0^{\mathrm{2D}} \cap A)$ represents the intersections of the secondary line sources with the listening area, that is $\mathbf{x}_0^{\mathrm{A}} \in x_0$ holds. In that case, a correction term must be applied (Vogel 1993, equations 3.5.15 and 3.5.19, Spors et al. 2008, equation 24). Since in that case 2D WFS is carried out with 3D secondary sources, the procedure is referred to as 2.5D WFS (Start et al. 1997, Spors et al. 2008). 2.5D WFS is described based on equation 30 by replacing the 2D free space Green's functions by secondary source corrected 3D free space Green's functions and the gradients of the 2D Green's functions by corrected 3D gradients.

In the following, the complex-valued, frequency dependent correction factors $C_{\mathrm{ss},G}(\mathbf{x}_{\mathrm{ref,ssc}}^{\mathrm{A}}|\mathbf{x}_0^{\mathrm{A}})$ and $C_{\mathrm{ss},\partial G}(\mathbf{x}_{\mathrm{ref,ssc}}^{\mathrm{A}}|\mathbf{x}_0^{\mathrm{A}})$ are referred to as secondary source correction (SSC) factors, valid with respect to the reference point $\mathbf{x}_{\mathrm{ref,ssc}}^{\mathrm{A}} \in (A \setminus x_0)$. Secondary source corrections have been proposed in approximate form (Vogel 1993, Start 1997, Spors et al. 2008, some derived with the *stationary phase approximation*). Here, a more general definition is given, with equations 3 and 28 for secondary monopole sources by

$$
\begin{aligned}
C_{\mathrm{ss},G}(\mathbf{x}_{\mathrm{ref,ssc}}^{\mathrm{A}}|\mathbf{x}_0^{\mathrm{A}}) &= \frac{G_{\mathrm{2D}}(\mathbf{x}_{\mathrm{ref,ssc}}^{\mathrm{A}}|\mathbf{x}_0^{\mathrm{A}})}{G_{\mathrm{3D}}(\mathbf{x}_{\mathrm{ref,ssc}}^{\mathrm{A}}|\mathbf{x}_0^{\mathrm{A}})} \\
&= \left|\mathbf{x}_{\mathrm{ref,ssc}}^{\mathrm{A}} - \mathbf{x}_0^{\mathrm{A}}\right| \mathrm{e}^{\mathrm{j}\left(k\left|\mathbf{x}_{\mathrm{ref,ssc}}^{\mathrm{A}} - \mathbf{x}_0^{\mathrm{A}}\right| - \frac{\pi}{2}\right)} \times \\
&\quad \times \pi H_0^{(2)}\left(k\left|\mathbf{x}_{\mathrm{ref,ssc}}^{\mathrm{A}} - \mathbf{x}_0^{\mathrm{A}}\right|\right), \\
&\qquad \forall\left(k\left|\mathbf{x}_{\mathrm{ref,ssc}}^{\mathrm{A}} - \mathbf{x}_0^{\mathrm{A}}\right|\right) > 0,
\end{aligned}
\tag{35}
$$

and with equations 3, 5, and 29 for secondary dipole sources by

$$
\begin{aligned}
C_{\mathrm{ss},\partial G}(\mathbf{x}_{\mathrm{ref,ssc}}^{\mathrm{A}}|\mathbf{x}_0^{\mathrm{A}}) &= \frac{\frac{\partial}{\partial \mathbf{n}} G_{\mathrm{2D}}(\mathbf{x}_{\mathrm{ref,ssc}}^{\mathrm{A}}|\mathbf{x}_0^{\mathrm{A}})}{\frac{\partial}{\partial \mathbf{n}} G_{\mathrm{3D}}(\mathbf{x}_{\mathrm{ref,ssc}}^{\mathrm{A}}|\mathbf{x}_0^{\mathrm{A}})} \\
&= \frac{\left|\mathbf{x}_{\mathrm{ref,ssc}}^{\mathrm{A}} - \mathbf{x}_0^{\mathrm{A}}\right|^2}{1 + \mathrm{j}k\left|\mathbf{x}_{\mathrm{ref,ssc}}^{\mathrm{A}} - \mathbf{x}_0^{\mathrm{A}}\right|} \mathrm{e}^{\mathrm{j}\left(k\left|\mathbf{x}_{\mathrm{ref,ssc}}^{\mathrm{A}} - \mathbf{x}_0^{\mathrm{A}}\right| - \frac{\pi}{2}\right)} \times \\
&\quad \times k\pi H_1^{(2)}\left(k\left|\mathbf{x}_{\mathrm{ref,ssc}}^{\mathrm{A}} - \mathbf{x}_0^{\mathrm{A}}\right|\right), \\
&\qquad \forall\left(k\left|\mathbf{x}_{\mathrm{ref,ssc}}^{\mathrm{A}} - \mathbf{x}_0^{\mathrm{A}}\right|\right) > 0.
\end{aligned}
\tag{36}
$$

The pressure spectrum of the 3D field generated by 2.5D WFS is computed based on equation 30 using equations 35 and 36 to replace the Green's functions $G_{\mathrm{2D}}(\mathbf{x}^{\mathrm{2D}}|\mathbf{x}_0^{\mathrm{2D}})$ by $G_{\mathrm{3D}}(\mathbf{x}|\mathbf{x}_0^{\mathrm{A}})\,C_{\mathrm{ss},G}(\mathbf{x}_{\mathrm{ref,ssc}}^{\mathrm{A}}|\mathbf{x}_0^{\mathrm{A}})$ and their directional gradients $\frac{\partial}{\partial \mathbf{n}} G_{\mathrm{2D}}(\mathbf{x}^{\mathrm{2D}}|\mathbf{x}_0^{\mathrm{2D}})$ by $\frac{\partial}{\partial \mathbf{n}} G_{\mathrm{3D}}(\mathbf{x}|\mathbf{x}_0^{\mathrm{A}})\,C_{\mathrm{ss},\partial G}(\mathbf{x}_{\mathrm{ref,ssc}}^{\mathrm{A}}|\mathbf{x}_0^{\mathrm{A}})$, resulting in

$$
\begin{aligned}
P_{\mathrm{2.5D}}&(\mathbf{x}|\mathbf{x}_{\mathrm{ref,ssc}}^{\mathrm{A}}) = \\
&= -\oint_{x_0} \Bigg[G_{\mathrm{3D}}(\mathbf{x}|\mathbf{x}_0^{\mathrm{A}})\,C_{\mathrm{ss},G}(\mathbf{x}_{\mathrm{ref,ssc}}^{\mathrm{A}}|\mathbf{x}_0^{\mathrm{A}}) \times - \\
&\quad \times \frac{\partial}{\partial \mathbf{n}} P(\mathbf{x}_0^{\mathrm{2D}}) - P(\mathbf{x}_0^{\mathrm{2D}})\frac{\partial}{\partial \mathbf{n}} G_{\mathrm{3D}}(\mathbf{x}|\mathbf{x}_0^{\mathrm{A}}) \times \\
&\quad \times C_{\mathrm{ss},\partial G}(\mathbf{x}_{\mathrm{ref,ssc}}^{\mathrm{A}}|\mathbf{x}_0^{\mathrm{A}}) \Bigg] dx_0,
\end{aligned}
\tag{37}
$$

$$
\forall \mathbf{x} \in (A \setminus x_0),\ \mathbf{x}_{\mathrm{ref,ssc}}^{\mathrm{A}} \in (A \setminus x_0),
$$
$$
\mathbf{x}_0^{\mathrm{A}} \in x_0,\ \mathbf{x}_0^{\mathrm{A}} = (\mathbf{x}_0^{\mathrm{2D}} \cap A),\ k > 0.
$$

The sound field represented by equation 37 equals the intended field exclusively at the reference point $\mathbf{x}_{\mathrm{ref,ssc}}^{\mathrm{A}}$. In general, no Cartesian coordinate system can be found where the field given by equation 37 is independent of one coordinate direction.

This paper was presented at the 133$^{\mathrm{rd}}$ Convention of the Audio Engineering Society 2012, as paper number 8717.

Page 10 of 20

7. PRIMARY SOURCE CORRECTION IN 2.5D WAVE FIELD SYNTHESIS

The PSC proposed for 2D WFS is directly applicable to 2.5D WFS because of its independence of the secondary sources and their positions. Therefore, the 2.5D WFS of a primary cylindrical wave with PSC is given using equations 11, 18, 33, and 37 by

$$
P_{\mathrm{sw,psc,2.5D}}(\mathbf{x}|\mathbf{x}_{\mathrm{ref,ssc}}^{\mathrm{A}}|\mathbf{x}_{\mathrm{ref,psc}}^{\mathrm{A}}|\mathbf{x}_{\mathrm{p}}^{\mathrm{A}}) =
$$

$$
= -\oint_{x_0} \bigg[G_{\mathrm{3D}}(\mathbf{x}|\mathbf{x}_0^{\mathrm{A}})\, C_{\mathrm{ss},G}(\mathbf{x}_{\mathrm{ref,ssc}}^{\mathrm{A}}|\mathbf{x}_0^{\mathrm{A}}) \times
$$

$$
\times \frac{\partial}{\partial \mathbf{n}} P_{\mathrm{cw}}(\mathbf{x}_0^{\mathrm{2D}}|\mathbf{x}_{\mathrm{p}}^{\mathrm{2D}}) - P_{\mathrm{cw}}(\mathbf{x}_0^{\mathrm{2D}}|\mathbf{x}_{\mathrm{p}}^{\mathrm{2D}}) \times
$$

$$
\times \frac{\partial}{\partial \mathbf{n}} G_{\mathrm{3D}}(\mathbf{x}|\mathbf{x}_0^{\mathrm{A}})\, C_{\mathrm{ss},\partial G}(\mathbf{x}_{\mathrm{ref,ssc}}^{\mathrm{A}}|\mathbf{x}_0^{\mathrm{A}}) \bigg] dx_0 \times \quad (38)
$$

$$
\times C_{\mathrm{ps}}(\mathbf{x}_{\mathrm{ref,psc}}^{\mathrm{A}}|\mathbf{x}_{\mathrm{p}}^{\mathrm{A}}),
$$

$$
\forall \mathbf{x} \in (A \setminus x_0),\; \mathbf{x}_{\mathrm{ref,psc}}^{\mathrm{A}}, \mathbf{x}_{\mathrm{ref,ssc}}^{\mathrm{A}} \in (A \setminus x_0),
$$

$$
\mathbf{x}_0^{\mathrm{A}} \in x_0,\; \mathbf{x}_{\mathrm{p}}^{\mathrm{2D}}, \mathbf{x}_{\mathrm{p}}^{\mathrm{A}} \notin (A \cup x_0),
$$

$$
\mathbf{x}_0^{\mathrm{A}} = (\mathbf{x}_0^{\mathrm{2D}} \cap A),\; k > 0.
$$

Equation 38 may be simplified by selecting identical reference points for primary and secondary source correction $\mathbf{x}_{\mathrm{ref,psc}}^{\mathrm{A}} = \mathbf{x}_{\mathrm{ref,ssc}}^{\mathrm{A}}$.

8. WAVE FIELD SYNTHESIS WITH SECONDARY MONOPOLE SOURCES ONLY

Copley (1968) showed that the control over the sound pressure field within a listening volume can be achieved using a secondary monopole distribution on the listening volume surface S_0. This procedure is according to Williams (1999) referred to as *simple source formulation.*

Another mathematically correct approach to discard one of the contributions to the KHI (monopole or dipole sources) is to use Green's functions equaling zero on S_0 or showing a directional gradient in boundary normal direction equal to zero on S_0 (Dirichlet respectively Neumann Green's functions, cf. Williams 1999).

In WFS, typically a for arbitrary configurations approximate approach is employed to reduce the situation to the monopole only case (Spors et al. 2008, p. 4). It can be shown that

$$
G_{\mathrm{N,p}}(\mathbf{x}|\mathbf{x}_0) = 2\, G_{\mathrm{3D}}(\mathbf{x}|\mathbf{x}_0) \qquad \text{and} \qquad (39)
$$

$$
G_{\mathrm{N,l}}(\mathbf{x}^{\mathrm{2D}}|\mathbf{x}_0^{\mathrm{2D}}) = 2\, G_{\mathrm{2D}}(\mathbf{x}^{\mathrm{2D}}|\mathbf{x}_0^{\mathrm{2D}}) \qquad (40)
$$

represent Neumann Green's functions for planar respectively linear boundaries S_0 or x_0 (Williams 1999, section 8.8.3). This holds not true for arbitrarily shaped boundaries. However, the artifacts resulting from applying $G_{\mathrm{N,p}}(\mathbf{x}|\mathbf{x}_0)$ or $G_{\mathrm{N,l}}(\mathbf{x}^{\mathrm{2D}}|\mathbf{x}_0^{\mathrm{2D}})$ and thereby the assumption of Neumann boundary conditions on S_0 or x_0 to arbitrarily shaped boundaries can be reduced by deactivating secondary sources at positions $\mathbf{x}_0$ where the local propagation direction $\mathbf{n}_{\mathrm{pf}}(\mathbf{x}_0)$ of the primary field (cf. section 3) exhibits no positive component in the direction of the boundary normal $\mathbf{n}(\mathbf{x}_0)$ (Spors 2007a).

The secondary source deactivation is carried out by multiplication of the sound pressure gradients by the so-called secondary source activation factors

$$
a(\mathbf{x}_0) = \begin{cases} 1 & \text{if } \langle \mathbf{n}_{\mathrm{pf}}(\mathbf{x}_0), \mathbf{n}(\mathbf{x}_0) \rangle > 0, \\ 0 & \text{otherwise}, \end{cases} \quad (41)
$$

defined here in principle according to Spors (2007a,b), but based on geometrical criteria rather than the primary field intensity vector.

Discarding the secondary dipole sources combined with the deactivation procedure results in general in two major consequences: a sound field outside the listening area or listening volume arises, and the field inside the listening area or volume deviates from the primary field (Spors et al. 2008, p. 5). To ensure that no contributions of the erroneous outer field propagate into the listening area or volume and interfere with the field created intentionally, convex listening area or volume boundaries are required then.

In principle, comparable simplifications are possible to allow for approximately correct dipole only WFS (Verheijen 1997). However, typical implementations are based on the monopole only theory (Verheijen 1997, Spors et al. 2008), since closed loudspeaker boxes resemble more closely monopole characteristics, especially at low frequencies where usually no alias artifacts occur (Zollner and Zwicker 1993).

In the following, monopole only WFS is discussed for 3D, 2D, and 2.5D situations, including the derivation of driving functions $D(\mathbf{x}_0)$ for the synthesis of plane and spherical primary fields. The driving functions represent the spectra of the signals the secondary monopole sources must be driven by to approximate the targeted primary sound field.

This paper was presented at the 133rd Convention of the Audio Engineering Society 2012, as paper number 8717.

Page 11 of 20

8.1. 3D Monopole Only Wave Field Synthesis

Based on equation 2, 3D WFS within the volume V bounded by S_0 using secondary monopole sources at $\mathbf{x}_0 \in S_0$ only is at $\mathbf{x} \in V$ described by the pressure field spectrum

$$
\begin{aligned}
P(\mathbf{x}) &= \oiint_{S_0} -2a(\mathbf{x}_0)G_{3\mathrm{D}}(\mathbf{x}|\mathbf{x}_0)\frac{\partial}{\partial\mathbf{n}}P(\mathbf{x}_0)dS_0 \\
&= \oiint_{S_0} D_{3\mathrm{D}}(\mathbf{x}_0)G_{3\mathrm{D}}(\mathbf{x}|\mathbf{x}_0)dS_0,
\end{aligned}
\tag{42}
$$
$$
\forall\, \mathbf{x} \neq \mathbf{x}_0.
$$

Here, $D_{3\mathrm{D}}(\mathbf{x}_0)$ represents the driving functions for 3D monopole only WFS, given by

$$
D_{3\mathrm{D}}(\mathbf{x}_0) = -2a(\mathbf{x}_0)\frac{\partial}{\partial\mathbf{n}}P(\mathbf{x}_0).
\tag{43}
$$

8.2. 2D Monopole Only Wave Field Synthesis

Using equation 30, the spectrum of the pressure field resulting from 2D WFS with secondary monopole line sources at $\mathbf{x}_0^{2\mathrm{D}} \in x_0$ only is given for two-dimensional primary fields at $\mathbf{x}^{2\mathrm{D}} \in A$ by

$$
\begin{aligned}
P(\mathbf{x}^{2\mathrm{D}}) &= \oint_{x_0} -2a(\mathbf{x}_0^{2\mathrm{D}})G_{2\mathrm{D}}(\mathbf{x}^{2\mathrm{D}}|\mathbf{x}_0^{2\mathrm{D}})\times \\
&\qquad \times \frac{\partial}{\partial\mathbf{n}}P(\mathbf{x}_0^{2\mathrm{D}})dx_0 \\
&= \oint_{x_0} D_{2\mathrm{D}}(\mathbf{x}_0^{2\mathrm{D}})G_{2\mathrm{D}}(\mathbf{x}^{2\mathrm{D}}|\mathbf{x}_0^{2\mathrm{D}})dx_0\,,
\end{aligned}
\tag{44}
$$
$$
\forall\, \mathbf{x}^{2\mathrm{D}} \neq \mathbf{x}_0^{2\mathrm{D}}.
$$

The driving functions for 2D monopole only WFS are defined by

$$
D_{2\mathrm{D}}(\mathbf{x}_0^{2\mathrm{D}}) = -2a(\mathbf{x}_0^{2\mathrm{D}})\frac{\partial}{\partial\mathbf{n}}P(\mathbf{x}_0^{2\mathrm{D}}).
\tag{45}
$$

Conventional 2D WFS is only capable of correctly reproducing sound fields independent of the coordinate direction given by the axes of the secondary line sources (that is perpendicular to the listening area, cf. section 4).

For the synthesis of a primary point source at $\mathbf{x}_\mathrm{p}^{\mathrm{A}}$ in the plane defined by the listening area A, PSC with respect to the reference point $\mathbf{x}_{\mathrm{ref,psc}}^{\mathrm{A}}$ within the listening area is applied to 2D monopole only WFS (cf. section 5).

The resulting pressure field spectrum is given according to equation 34 by

$$
\begin{aligned}
P_{\mathrm{sw,psc,2D}}&(\mathbf{x}^{2\mathrm{D}}|\mathbf{x}_{\mathrm{ref,psc}}^{\mathrm{A}}|\mathbf{x}_\mathrm{p}^{\mathrm{A}}) = \\
&= \oint_{x_0} -2a(\mathbf{x}_0^{2\mathrm{D}})G_{2\mathrm{D}}(\mathbf{x}^{2\mathrm{D}}|\mathbf{x}_0^{2\mathrm{D}})\times \\
&\quad \times \frac{\partial}{\partial\mathbf{n}}P_{\mathrm{cw}}(\mathbf{x}_0^{2\mathrm{D}}|\mathbf{x}_\mathrm{p}^{\mathrm{A}})dx_0\, C_{\mathrm{ps}}(\mathbf{x}_{\mathrm{ref,psc}}^{\mathrm{A}}|\mathbf{x}_\mathrm{p}^{\mathrm{A}}) \\
&= \oint_{x_0} D_{\mathrm{2D,sw,psc}}(\mathbf{x}_0^{2\mathrm{D}}|\mathbf{x}_{\mathrm{ref,psc}}^{\mathrm{A}}|\mathbf{x}_\mathrm{p}^{\mathrm{A}})\times \\
&\quad \times G_{2\mathrm{D}}(\mathbf{x}^{2\mathrm{D}}|\mathbf{x}_0^{2\mathrm{D}})dx_0,
\end{aligned}
\tag{46}
$$
$$
\forall\, \mathbf{x}^{2\mathrm{D}} \neq \mathbf{x}_0^{2\mathrm{D}},\, \left(k\left|\mathbf{x}_{\mathrm{ref,psc}}^{\mathrm{A}} - \mathbf{x}_\mathrm{p}^{\mathrm{A}}\right|\right) > 0.
$$

The pressure field represented by equation 46 equals the primary spherical pressure field exclusively at the reference position $\mathbf{x}_\mathrm{p}^{\mathrm{A}}$. The corresponding driving functions are given by

$$
\begin{aligned}
D_{\mathrm{2D,sw,psc}}&(\mathbf{x}_0^{2\mathrm{D}}|\mathbf{x}_{\mathrm{ref,psc}}^{\mathrm{A}}|\mathbf{x}_\mathrm{p}^{\mathrm{A}}) = \\
&= -2a(\mathbf{x}_0^{2\mathrm{D}})\, C_{\mathrm{ps}}(\mathbf{x}_{\mathrm{ref,psc}}^{\mathrm{A}}|\mathbf{x}_\mathrm{p}^{\mathrm{A}})\frac{\partial}{\partial\mathbf{n}}P_{\mathrm{cw}}(\mathbf{x}_0^{2\mathrm{D}}|\mathbf{x}_\mathrm{p}^{\mathrm{A}}).
\end{aligned}
\tag{47}
$$

8.3. 2.5D Monopole Only Wave Field Synthesis

Equation 37 can be adapted to represent 2.5D monopole only WFS with the reference point $\mathbf{x}_{\mathrm{ref,ssc}}^{\mathrm{A}}$ in the listening area A by

$$
\begin{aligned}
P_{2.5\mathrm{D}}(\mathbf{x}|\mathbf{x}_{\mathrm{ref,ssc}}^{\mathrm{A}}) &= \oint_{x_0} -2a(\mathbf{x}_0^{\mathrm{A}})G_{3\mathrm{D}}(\mathbf{x}|\mathbf{x}_0^{\mathrm{A}})\times \\
&\quad \times C_{\mathrm{ss},G}(\mathbf{x}_{\mathrm{ref,ssc}}^{\mathrm{A}}|\mathbf{x}_0^{\mathrm{A}})\frac{\partial}{\partial\mathbf{n}}P(\mathbf{x}_0^{2\mathrm{D}})dx_0 \\
&= \oint_{x_0} D_{2.5\mathrm{D}}(\mathbf{x}_0^{\mathrm{A}}|\mathbf{x}_{\mathrm{ref,ssc}}^{\mathrm{A}})G_{3\mathrm{D}}(\mathbf{x}|\mathbf{x}_0^{\mathrm{A}})dx_0,
\end{aligned}
\tag{48}
$$
$$
\forall\, \mathbf{x} \neq \mathbf{x}_0^{\mathrm{A}},\, \left(k\left|\mathbf{x}_{\mathrm{ref,ssc}}^{\mathrm{A}} - \mathbf{x}_0^{\mathrm{A}}\right|\right) > 0.
$$

The driving functions for the 2.5D monopole only WFS are here defined by

$$
\begin{aligned}
D_{2.5\mathrm{D}}&(\mathbf{x}_0^{\mathrm{A}}|\mathbf{x}_{\mathrm{ref,ssc}}^{\mathrm{A}}) = \\
&= -2a(\mathbf{x}_0^{\mathrm{A}})\, C_{\mathrm{ss},G}(\mathbf{x}_{\mathrm{ref,ssc}}^{\mathrm{A}}|\mathbf{x}_0^{\mathrm{A}})\frac{\partial}{\partial\mathbf{n}}P(\mathbf{x}_0^{2\mathrm{D}}), \\
&\forall\, \left(k\left|\mathbf{x}_{\mathrm{ref,ssc}}^{\mathrm{A}} - \mathbf{x}_0^{\mathrm{A}}\right|\right) > 0.
\end{aligned}
\tag{49}
$$

Derived from 2D WFS, 2.5D monopole only WFS is also not capable of generating spherical waves or arbitrary 3D fields (section 6).

The 2.5D scenario with PSC optimized for the reference point $\mathbf{x}_{\mathrm{ref,ssc}}^{\mathrm{A}}$, simulating a primary spherical

This paper was presented at the 133rd Convention of the Audio Engineering Society 2012, as paper number 8717.

Page 12 of 20

wave generated by a point source at $\mathbf{x}_p^A$ within the listening area A, is derived from equation 38 to

$$
\begin{aligned}
P_{\mathrm{sw,psc,2.5D}}&(\mathbf{x}|\mathbf{x}_{\mathrm{ref,ssc}}^A|\mathbf{x}_{\mathrm{ref,psc}}^A|\mathbf{x}_p^A) = \\
&= \oint_{x_0} -2a(\mathbf{x}_0^A)C_{\mathrm{ps}}(\mathbf{x}_{\mathrm{ref,psc}}^A|\mathbf{x}_0^A)G_{\mathrm{3D}}(\mathbf{x}|\mathbf{x}_0^A) \times \\
&\qquad \times C_{\mathrm{ss},G}(\mathbf{x}_{\mathrm{ref,ssc}}^A|\mathbf{x}_0^A)\frac{\partial}{\partial\mathbf{n}}P_{\mathrm{cw}}(\mathbf{x}_0^{\mathrm{2D}}|\mathbf{x}_p^{\mathrm{2D}})dx_0 \\
&= \oint_{x_0} D_{\mathrm{2.5D,psc}}(\mathbf{x}_0^A|\mathbf{x}_p^A|\mathbf{x}_{\mathrm{ref,ssc}}^A|\mathbf{x}_{\mathrm{ref,psc}}^A) \times \\
&\qquad \times G_{\mathrm{3D}}(\mathbf{x}|\mathbf{x}_0^A)dx_0,
\end{aligned}
\tag{50}
$$

$$
\forall\, \mathbf{x} \neq \mathbf{x}_0^A, \left(k\left|\mathbf{x}_{\mathrm{ref,psc}}^A - \mathbf{x}_p^A\right|\right) > 0,
$$
$$
\left(k\left|\mathbf{x}_{\mathrm{ref,ssc}}^A - \mathbf{x}_0^A\right|\right) > 0.
$$

The primary and secondary source corrected 2.5D driving functions are then given by

$$
\begin{aligned}
D_{\mathrm{2.5D,psc}}&(\mathbf{x}_0^A|\mathbf{x}_p^A|\mathbf{x}_{\mathrm{ref,ssc}}^A|\mathbf{x}_{\mathrm{ref,psc}}^A) = \\
&= -2a(\mathbf{x}_0^A)\,C_{\mathrm{ss},G}(\mathbf{x}_{\mathrm{ref,ssc}}^A|\mathbf{x}_0^A) \times \\
&\quad \times C_{\mathrm{ps}}(\mathbf{x}_{\mathrm{ref,psc}}^A|\mathbf{x}_p^A)\frac{\partial}{\partial\mathbf{n}}P_{\mathrm{cw}}(\mathbf{x}_0^{\mathrm{2D}}|\mathbf{x}_p^{\mathrm{2D}}).
\end{aligned}
\tag{51}
$$

9. PREVIOUS APPROACHES
Previous approaches to WFS typically aim at implementing systems with monopole secondary sources only (Boone et al. 1995, Gauthier and Berry 2006, 2008, Spors et al. 2008). Consequently, the majority of driving functions available holds for that situation, and the comparison is restricted to the monopole only case here.

9.1. 2D Monopole Only Wave Field Synthesis
Spors et al. (2008, equation 17) define driving functions for plane waves in 3D and 2D WFS, given adapted to the nomenclature employed here by

$$
\begin{aligned}
D_{\mathrm{2D,pw,sp}}(\mathbf{x}_0^{\mathrm{2D}}) &= 2a(\mathbf{x}_0^{\mathrm{2D}})k\,e^{-j\left(k\mathbf{n}_{\mathrm{pw}}^{\mathrm{T}}\mathbf{x}_0^{\mathrm{2D}} - \frac{\pi}{2}\right)} \times \\
&\quad \times \mathbf{n}_{\mathrm{pw}}^{\mathrm{T}}\mathbf{n}(\mathbf{x}_0^{\mathrm{2D}})\hat{P}_a.
\end{aligned}
\tag{52}
$$

Note that with regard to the WFS implementation, the minus preceding the KHI is included in the driving function in this paper (comparable to Verheijen 1997), in contrast to Spors et al. (2008, equation 11). For that reason, the sign of equation 52 is inverted compared to equation 17 of Spors et al. (2008).

Based on equations 6, 7, and 45, it is possible to give the driving functions implementing the framework

derived here for the synthesis of primary plane waves with 2D WFS by

$$
\begin{aligned}
D_{\mathrm{2D,pw}}(\mathbf{x}_0^{\mathrm{2D}}) &= 2a(\mathbf{x}_0^{\mathrm{2D}})k\,e^{-j\left(k\mathbf{n}_{\mathrm{pw}}^{\mathrm{T}}\mathbf{x}_0^{\mathrm{2D}} - \frac{\pi}{2}\right)} \times \\
&\quad \times \mathbf{n}_{\mathrm{pw}}^{\mathrm{T}}\mathbf{n}(\mathbf{x}_0^{\mathrm{2D}})\hat{P}_a \\
&= D_{\mathrm{2D,pw,sp}}(\mathbf{x}_0^{\mathrm{2D}}).
\end{aligned}
\tag{53}
$$

The comparison to equation 52 reveals the identity of both formulae. In other words: the driving functions for plane waves in 2D WFS derived here are identical to those given by Spors et al. (2008).

Spherical primary fields cannot be synthesized correctly by 2D WFS (cf. section 4) without the PSC introduced here. For that reason, no comparison to previous approaches is given.

Driving functions for primary cylindrical fields in 2D WFS are given by Spors et al. (2008, equation 23, adapted to the nomenclature employed here) by

$$
\begin{aligned}
D_{\mathrm{2D,cw,sp}}(\mathbf{x}_0^{\mathrm{2D}}) &= \frac{a(\mathbf{x}_0^{\mathrm{2D}})}{2c}k\,e^{j\frac{\pi}{2}}\hat{P}_a \times \\
&\times H_1^{(2)}\left(k\left|\mathbf{x}_0^{\mathrm{2D}} - \mathbf{x}_p^{\mathrm{2D}}\right|\right)\frac{(\mathbf{x}_0^{\mathrm{2D}} - \mathbf{x}_p^{\mathrm{2D}})^{\mathrm{T}}\mathbf{n}(\mathbf{x}_0^{\mathrm{2D}})}{\left|\mathbf{x}_0^{\mathrm{2D}} - \mathbf{x}_p^{\mathrm{2D}}\right|}.
\end{aligned}
\tag{54}
$$

Again, the sign is inverted here to account for the different driving function definitions employed here and by Spors et al. (2008).

Combining equations 16, 18, and 45, the 2D driving functions for primary cylindrical waves derived here can be written by

$$
\begin{aligned}
D_{\mathrm{2D,cw}}(\mathbf{x}_0^{\mathrm{2D}}) &= 2\pi a(\mathbf{x}_0^{\mathrm{2D}})k\,e^{-j\frac{\pi}{2}}\hat{P}_a \times \\
&\times H_1^{(2)}\left(k\left|\mathbf{x}_0^{\mathrm{2D}} - \mathbf{x}_p^{\mathrm{2D}}\right|\right)\frac{(\mathbf{x}_0^{\mathrm{2D}} - \mathbf{x}_p^{\mathrm{2D}})^{\mathrm{T}}\mathbf{n}(\mathbf{x}_0^{\mathrm{2D}})}{\left|\mathbf{x}_0^{\mathrm{2D}} - \mathbf{x}_p^{\mathrm{2D}}\right|}, \\
&\forall\,\left(k\left|\mathbf{x}_0^{\mathrm{2D}} - \mathbf{x}_p^{\mathrm{2D}}\right|\right) > 0.
\end{aligned}
\tag{55}
$$

With equations 54 and 55, the deviation of the driving functions for the 2D WFS of cylindrical waves derived here and by Spors et al. (2008) is given by

$$
E_{\mathrm{2D,cw,sp}} = \frac{D_{\mathrm{2D,cw,sp}}(\mathbf{x}_0^{\mathrm{2D}})}{D_{\mathrm{2D,cw}}(\mathbf{x}_0^{\mathrm{2D}})} = \frac{e^{j\pi}}{4\pi c}.
\tag{56}
$$

This deviation means that the fields resulting from the 2D WFS of cylindrical primary waves as given by Spors et al. (2008) exhibit the frequency and position independent level error

$$
\begin{aligned}
\Delta L_{\mathrm{2D,cw,sp}} &= 20\log_{10}\left(\left|E_{\mathrm{2D,cw,sp}}\right|\right)\mathrm{dB} \\
&\approx -73\,\mathrm{dB},
\end{aligned}
\tag{57}
$$

This paper was presented at the 133ʳᵈ Convention of the Audio Engineering Society 2012, as paper number 8717.

Page 13 of 20

and additionally the frequency and position independent phase deviation

$$\Delta\varphi_{2D,cw,sp} = \arg\left(E_{2D,cw,sp}\right) = \pi. \qquad (58)$$

Since Spors et al. (2008) give no explicit derivation of their equation 23, the reason for the deviation cannot be clarified here. However, different definitions of the pressure field spectrum of a line source (cf. equation 11) are likely contributing.

9.2. 2.5D Monopole Only Wave Field Synthesis

Previously derived driving functions for the 2.5D monopole only WFS are based on the large-argument approximations of the Hankel functions (equations 14 and 15) for the secondary source correction, and are therefore known to produce synthesis errors at evaluation positions close to the secondary source contours and at low frequencies (Spors and Ahrens 2010). The approximations are valid only for large arguments, meaning for large $\left(k\left|\mathbf{x}_{ref,ssc}^{A} - \mathbf{x}_{0}^{A}\right|\right)$ here.

However, in practical implementations, especially if the real-time computation is required, the approximations are helpful. For that reason, the comparisons to previous approaches are given here implementing the primary and secondary source corrections proposed by equations 34 and 35 for the approaches introduced here using the Hankel functions (equations 12 and 13), but also using their large-argument approximations (equations 14 and 15).

9.2.1. Plane Primary Fields

Spors et al. (2008, equation 27) propose driving functions for the 2.5D WFS of primary plane wave, adapted to the nomenclature defined here given by

$$D_{2.5D,pw,sp}(\mathbf{x}_{0}^{A}|\mathbf{x}_{ref}^{A}) = 2a(\mathbf{x}_{0}^{A})\mathbf{n}_{pw}^{T}\mathbf{n}(\mathbf{x}_{0}^{A})\hat{P}_{a}\times$$
$$\times\ e^{-j\left(k\mathbf{n}_{pw}^{T}\mathbf{x}_{0}^{A} - \frac{\pi}{4}\right)}\sqrt{2\pi k\left|\mathbf{x}_{ref}^{A} - \mathbf{x}_{0}^{A}\right|}. \qquad (59)$$

The driving functions for the 2.5D WFS of plane waves derived in this paper are given with equations 7, 35, and 49 by

$$D_{2.5D,pw}(\mathbf{x}_{0}^{A}|\mathbf{x}_{ref,ssc}^{A}) = 2a(\mathbf{x}_{0}^{A})\mathbf{n}_{pw}^{T}\mathbf{n}(\mathbf{x}_{0}^{A})\hat{P}_{a}\times$$
$$\times\ \pi k\left|\mathbf{x}_{ref,ssc}^{A} - \mathbf{x}_{0}^{A}\right|H_{0}^{(2)}\left(k\left|\mathbf{x}_{ref,ssc}^{A} - \mathbf{x}_{0}^{A}\right|\right)\times$$
$$\times\ e^{-jk\left(\mathbf{n}_{pw}^{T}\mathbf{x}_{0}^{A} - \left|\mathbf{x}_{ref,ssc}^{A} - \mathbf{x}_{0}^{A}\right|\right)}, \qquad (60)$$
$$\forall\ \left(k\left|\mathbf{x}_{ref,ssc}^{A} - \mathbf{x}_{0}^{A}\right|\right) > 0.$$

Employing the large-argument approximation of the Hankel function of the second kind, zeroth order (equation 15), equation 60 can be written by

$$D_{2.5D,pw}(\mathbf{x}_{0}^{A}|\mathbf{x}_{ref,ssc}^{A}) \approx 2a(\mathbf{x}_{0}^{A})\mathbf{n}_{pw}^{T}\mathbf{n}(\mathbf{x}_{0}^{A})\hat{P}_{a}\times$$
$$\times\ \sqrt{2\pi k\left|\mathbf{x}_{ref,ssc}^{A} - \mathbf{x}_{0}^{A}\right|}\ e^{-j\left(k\mathbf{n}_{pw}^{T}\mathbf{x}_{0}^{A} - \frac{\pi}{4}\right)}$$
$$= D_{2.5D,pw,sp}(\mathbf{x}_{0}^{A}|\mathbf{x}_{ref,ssc}^{A}), \qquad (61)$$
$$\forall\ \left(k\left|\mathbf{x}_{ref,ssc}^{A} - \mathbf{x}_{0}^{A}\right|\right) \gg 1.$$

For high frequencies and large distances between reference point and secondary sources, the driving functions for the 2.5D WFS of plane waves derived here and by Spors et al. (2008) are identical.

Figure 3 shows the error of the 2.5D WFS according to equation 61 that is using the Hankel function's large argument approximation with a primary plane wave ($\mathbf{n}_{pw} = [-1\ 0\ 0]^{T}$), exemplary for a circular secondary source contour of 1.3 m radius, centered around the origin $\mathbf{x}_{a} = [0\ 0\ 0]^{T}$ of a Cartesian coordinate system (geometry of figures 1 and 2). Magnitude and group
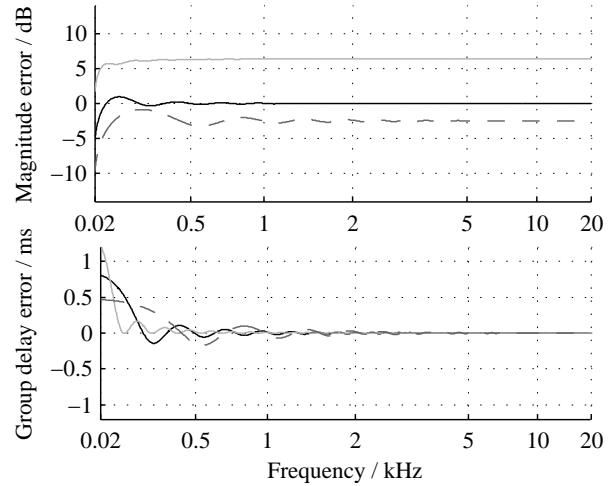

Fig. 3: Deviation of the pressure field created by 2.5D wave field synthesis of a plane wave with $\mathbf{n}_{pw} = [-1\ 0\ 0]^{T}$ using the large argument approximation of the Hankel function. Geometry and evaluation positions identical to figure 1.

delay errors are possibly audible, especially on head movements, considering the high temporal resolution of binaural hearing (Fastl and Zwicker 2007, p. 293).

This paper was presented at the 133rd Convention of the Audio Engineering Society 2012, as paper number 8717.

Page 14 of 20

9.2.2. Spherical Primary Fields

Early formulations of WFS are given specifically for linear or curved but infinitely extended secondary source contours (Vogel 1993, Start 1996, Verheijen 1997). However, WFS simulations or implementations require a finite integration region, introducing artifacts, which are typically reduced by applying a spatial truncation window (Start 1997, section 4). Since truncation methods are beyond the scope of this paper, the driving functions given by Verheijen (1997) are included in the comparison for 2.5D WFS, but applied to closed secondary source contours without truncation, using the secondary source activation factor given by equation 41. Expressing the cosine of the angle between the secondary source contour and the vector $\left(\mathbf{x}_0^{\mathrm{A}} - \mathbf{x}_{\mathrm{p}}^{\mathrm{A}}\right)$ by the scalar product of vector and contour normal, equation 2.32 b of Verheijen (1997) is given with equation 34 of Spors et al. (2008) and the nomenclature used here by

$$
\begin{aligned}
D_{2.5\mathrm{D,sw,ve}}(\mathbf{x}_0^{\mathrm{A}}|\mathbf{x}_{\mathrm{ref}}^{\mathrm{A}}) = {}& a(\mathbf{x}_0^{\mathrm{A}})\sqrt{\frac{k}{2\pi}}\hat{P}_{\mathrm{a}} \times \\
\times{}& \sqrt{\frac{|\mathbf{x}_{\mathrm{ref}}^{\mathrm{A}} - \mathbf{x}_0^{\mathrm{A}}|}{|\mathbf{x}_0^{\mathrm{A}} - \mathbf{x}_{\mathrm{p}}^{\mathrm{A}}| + |\mathbf{x}_{\mathrm{ref}}^{\mathrm{A}} - \mathbf{x}_0^{\mathrm{A}}|}} \times \\
\times{}& \frac{\mathrm{e}^{-\mathrm{j}\left(k|\mathbf{x}_0^{\mathrm{A}} - \mathbf{x}_{\mathrm{p}}^{\mathrm{A}}| - \frac{\pi}{4}\right)}}{\sqrt{|\mathbf{x}_0^{\mathrm{A}} - \mathbf{x}_{\mathrm{p}}^{\mathrm{A}}|}} \frac{(\mathbf{x}_0^{\mathrm{A}} - \mathbf{x}_{\mathrm{p}}^{\mathrm{A}})^{\mathrm{T}}\mathbf{n}(\mathbf{x}_0^{\mathrm{A}})}{|\mathbf{x}_0^{\mathrm{A}} - \mathbf{x}_{\mathrm{p}}^{\mathrm{A}}|}.
\end{aligned}
\tag{62}
$$

Figure 4 shows the error of the synthesis of spherical primary fields by 2.5D WFS using equation 62 for the geometry and evaluation positions of figure 1.

Magnitude and group delay errors are approximately frequency independent and vanish at the reference point for frequencies above some 500 Hz, apart from a global offset of about −22 dB, corresponding to the factor $1/(4\pi)$. At lower frequencies and off the reference point, frequency dependent errors occur.

The lower panel shows the average level error in the frequency range between 1 kHz and 5 kHz over the distance between primary source and origin. At the reference point, no primary source position dependent error occurs for distances larger than about 1.5 m. Away from the reference point, for primary sources close to the secondary source contour, and for focus points in general, distance dependent errors occur. The light gray line is shown for all distances, while the fields of focus points are not correct between
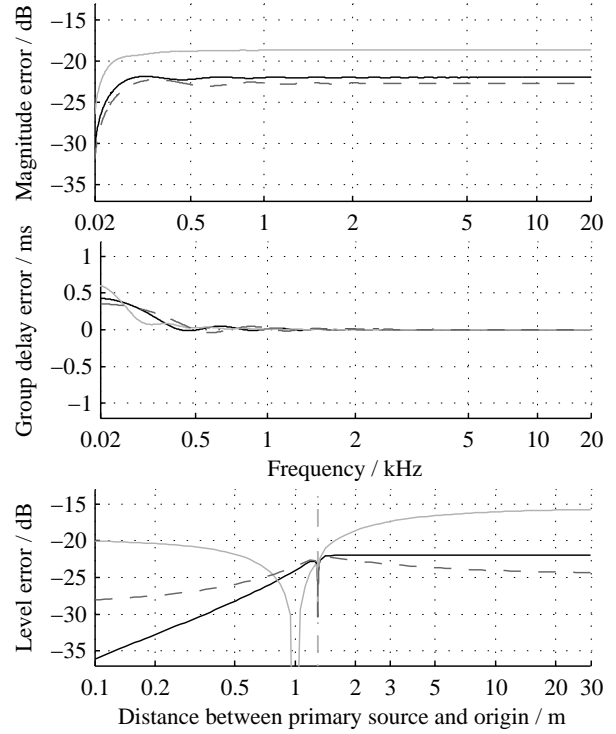

Fig. 4: Deviation of the pressure field created by 2.5D wave field synthesis according to Verheijen (1997, with modifications) from the targeted spherical field. Geometry and evaluation positions identical to figure 1.

secondary source contour and focus point, which is below 1 m here.

Equation 29 by Spors et al. (2008) represents another driving function for the 2.5D WFS of spherical primary fields, derived introducing a primary spherical field in the 2D KHI. According to section 4, this procedure is expected to result in erroneous fields. Using the nomenclature introduced here, Spors' driving functions are given by

$$
\begin{aligned}
D_{2.5\mathrm{D,sw,sp}}(\mathbf{x}_0^{\mathrm{A}}|\mathbf{x}_{\mathrm{ref}}^{\mathrm{A}}) = {}& 2a(\mathbf{x}_0^{\mathrm{A}})\hat{P}_{\mathrm{a}} \times \\
\times{}& \left(\frac{1}{\mathrm{j}k\left|\mathbf{x}_0^{\mathrm{A}} - \mathbf{x}_{\mathrm{p}}^{\mathrm{A}}\right|} + 1\right)\sqrt{\frac{2\pi k\left|\mathbf{x}_{\mathrm{ref}}^{\mathrm{A}} - \mathbf{x}_0^{\mathrm{A}}\right|}{\left|\mathbf{x}_0^{\mathrm{A}} - \mathbf{x}_{\mathrm{p}}^{\mathrm{A}}\right|}} \times \\
\times{}& \frac{\mathrm{e}^{-\mathrm{j}\left(k|\mathbf{x}_0^{\mathrm{A}} - \mathbf{x}_{\mathrm{p}}^{\mathrm{A}}| - \frac{\pi}{4}\right)}}{\sqrt{\left|\mathbf{x}_0^{\mathrm{A}} - \mathbf{x}_{\mathrm{p}}^{\mathrm{A}}\right|}} \frac{(\mathbf{x}_0^{\mathrm{A}} - \mathbf{x}_{\mathrm{p}}^{\mathrm{A}})^{\mathrm{T}}\mathbf{n}(\mathbf{x}_0^{\mathrm{A}})}{\left|\mathbf{x}_0^{\mathrm{A}} - \mathbf{x}_{\mathrm{p}}^{\mathrm{A}}\right|}.
\end{aligned}
\tag{63}
$$

Figure 5 shows the corresponding errors for the exemplary configuration used here.

This paper was presented at the 133$^{\mathrm{rd}}$ Convention of the Audio Engineering Society 2012, as paper number 8717.
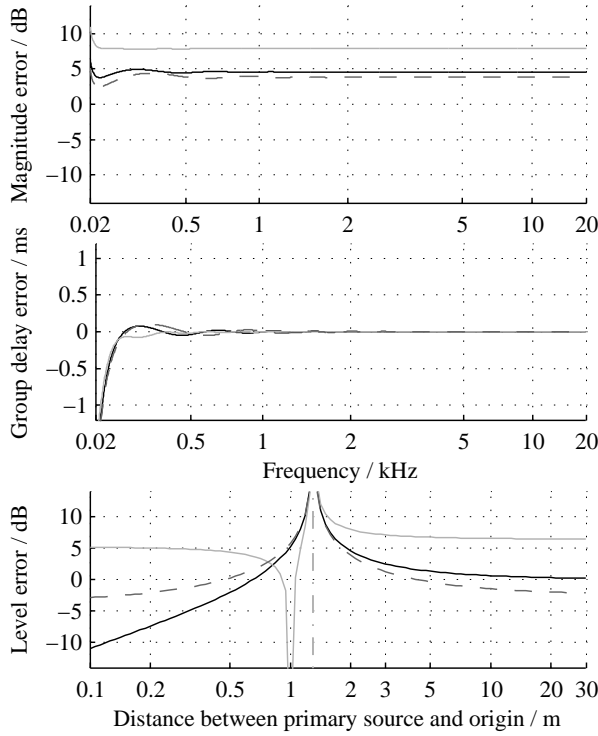
Page 15 of 20

Fig. 5: Deviation of the pressure field created by 2.5D WFS according to Spors et al. (2008) from the targeted spherical field. Geometry identical to figure 1.
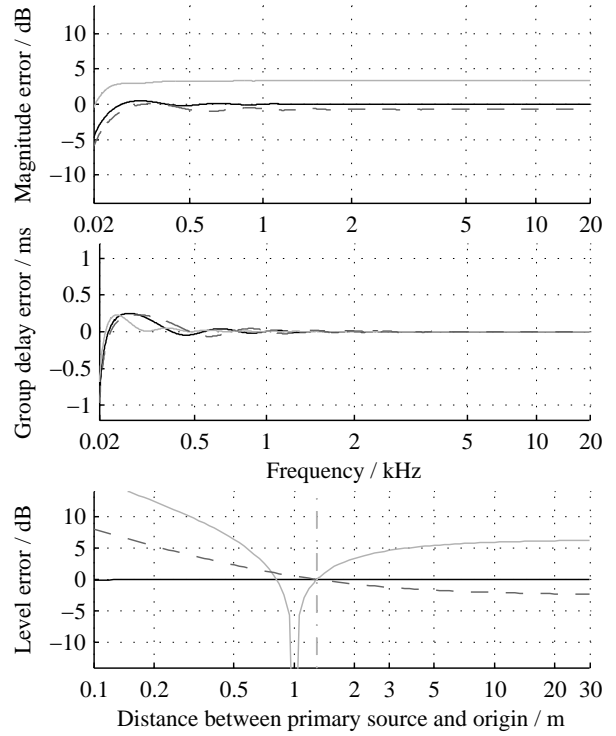
Fig. 6: Deviation of the pressure field created by 2.5D WFS with a cylindrical primary field and the primary source correction (PSC) introduced here from the targeted spherical field. Geometry identical to figure 1.

At all evaluation positions, a frequency independent but position dependent level error occurs in addition to low frequency deviations. The average level error depends on the primary source distance, with a pole for primary sources at the secondary source contour.

With equations 16, 18, 33, 35, and 51, the 2.5D WFS of a primary point source is given based on the framework introduced here by

$$
\begin{aligned}
D_{2.5\mathrm{D,psc}}&(\mathbf{x}_0^{\mathrm{A}}|\mathbf{x}_{\mathrm{p}}^{\mathrm{A}}|\mathbf{x}_{\mathrm{ref,ssc}}^{\mathrm{A}}|\mathbf{x}_{\mathrm{ref,psc}}^{\mathrm{A}}) = 2a(\mathbf{x}_0^{\mathrm{A}})\hat{P}_{\mathrm{a}}\times \\
&\times k\pi \frac{\mathrm{e}^{-\mathrm{j}\left(k\left|\mathbf{x}_{\mathrm{ref,psc}}^{\mathrm{A}}-\mathbf{x}_{\mathrm{p}}^{\mathrm{A}}\right|-k\left|\mathbf{x}_{\mathrm{ref,ssc}}^{\mathrm{A}}-\mathbf{x}_0^{\mathrm{A}}\right|+\frac{\pi}{2}\right)}}{\left|\mathbf{x}_{\mathrm{ref,psc}}^{\mathrm{A}}-\mathbf{x}_{\mathrm{p}}^{\mathrm{A}}\right|}\times \\
&\times \left|\mathbf{x}_{\mathrm{ref,ssc}}^{\mathrm{A}}-\mathbf{x}_0^{\mathrm{A}}\right| \frac{H_0^{(2)}\left(k\left|\mathbf{x}_{\mathrm{ref,ssc}}^{\mathrm{A}}-\mathbf{x}_0^{\mathrm{A}}\right|\right)}{H_0^{(2)}\left(k\left|\mathbf{x}_{\mathrm{ref,psc}}^{\mathrm{A}}-\mathbf{x}_{\mathrm{p}}^{\mathrm{A}}\right|\right)}\times \\
&\times H_1^{(2)}\left(k\left|\mathbf{x}_0^{\mathrm{A}}-\mathbf{x}_{\mathrm{p}}^{\mathrm{A}}\right|\right)\frac{(\mathbf{x}_0^{\mathrm{A}}-\mathbf{x}_{\mathrm{p}}^{\mathrm{A}})^{\mathrm{T}}\mathbf{n}(\mathbf{x}_0^{\mathrm{A}})}{\left|\mathbf{x}_0^{\mathrm{A}}-\mathbf{x}_{\mathrm{p}}^{\mathrm{A}}\right|}, \\
&\forall \left(k\left|\mathbf{x}_{\mathrm{ref,psc}}^{\mathrm{A}}-\mathbf{x}_{\mathrm{p}}^{\mathrm{A}}\right|\right) > 0, \\
&\left(k\left|\mathbf{x}_{\mathrm{ref,ssc}}^{\mathrm{A}}-\mathbf{x}_0^{\mathrm{A}}\right|\right) > 0, \left(k\left|\mathbf{x}_0^{\mathrm{A}}-\mathbf{x}_{\mathrm{p}}^{\mathrm{A}}\right|\right) > 0.
\end{aligned}
\tag{64}
$$

Figure 6 shows the errors resulting from the 2.5D WFS of a primary point source using the method derived here, with the reference point at the origin ($\mathbf{x}_{\mathrm{ref}}^{\mathrm{A}} = \mathbf{x}_{\mathrm{ref,psc}}^{\mathrm{A}} = \mathbf{x}_{\mathrm{ref,ssc}}^{\mathrm{A}} = [0\ 0\ 0]^{\mathrm{T}}$).

At the reference point, magnitude and group delay errors occur at frequencies below approximately $500\,\mathrm{Hz}$ due to the approximated Neumann Green's function (cf. equation 40).

The average level in the frequency range between $1\,\mathrm{kHz}$ and $5\,\mathrm{kHz}$ is correct at the reference point for all distances to the primary source, especially not exhibiting the pole for primary sources at the secondary source contour resulting from the method proposed by Spors et al. (2008). Off the reference point, distance dependent level errors occur.

Assuming the same reference points for primary and secondary source correction ($\mathbf{x}_{\mathrm{ref}}^{\mathrm{A}} = \mathbf{x}_{\mathrm{ref,psc}}^{\mathrm{A}} = \mathbf{x}_{\mathrm{ref,ssc}}^{\mathrm{A}}$) and employing the large-argument approximations of

This paper was presented at the 133rd Convention of the Audio Engineering Society 2012, as paper number 8717.

Page 16 of 20

the Hankel functions of the second kind (equation 15), equation 64 can be written by

$$D_{2.5\mathrm{D,sw}}(\mathbf{x}_0^{\mathrm{A}}|\mathbf{x}_{\mathrm{ref}}^{\mathrm{A}}) \approx$$

$$\approx 2a(\mathbf{x}_0^{\mathrm{A}}) \sqrt{\frac{2\pi k \left|\mathbf{x}_{\mathrm{ref}}^{\mathrm{A}} - \mathbf{x}_0^{\mathrm{A}}\right|}{\left|\mathbf{x}_{\mathrm{ref}}^{\mathrm{A}} - \mathbf{x}_{\mathrm{p}}^{\mathrm{A}}\right|}} \times$$

$$\times \frac{\mathrm{e}^{-\mathrm{j}\left(k\left|\mathbf{x}_0^{\mathrm{A}}-\mathbf{x}_{\mathrm{p}}^{\mathrm{A}}\right|-\frac{\pi}{4}\right)}}{\sqrt{\left|\mathbf{x}_0^{\mathrm{A}} - \mathbf{x}_{\mathrm{p}}^{\mathrm{A}}\right|}} \frac{(\mathbf{x}_0^{\mathrm{A}} - \mathbf{x}_{\mathrm{p}}^{\mathrm{A}})^{\mathrm{T}}\mathbf{n}(\mathbf{x}_0^{\mathrm{A}})}{\left|\mathbf{x}_0^{\mathrm{A}} - \mathbf{x}_{\mathrm{p}}^{\mathrm{A}}\right|} \hat{P}_{\mathrm{a}}, \quad (65)$$

$$\forall \left(k\left|\mathbf{x}_{\mathrm{ref}}^{\mathrm{A}} - \mathbf{x}_{\mathrm{p}}^{\mathrm{A}}\right|\right) > 0, \left(k\left|\mathbf{x}_{\mathrm{ref}}^{\mathrm{A}} - \mathbf{x}_0^{\mathrm{A}}\right|\right) > 0,$$
$$\left(k\left|\mathbf{x}_0^{\mathrm{A}} - \mathbf{x}_{\mathrm{p}}^{\mathrm{A}}\right|\right) > 0.$$

Figure 7 shows the errors resulting for the 2.5D WFS of a primary point source using the method derived here with the Hankel functions' large-argument approximations (reference point at the origin).
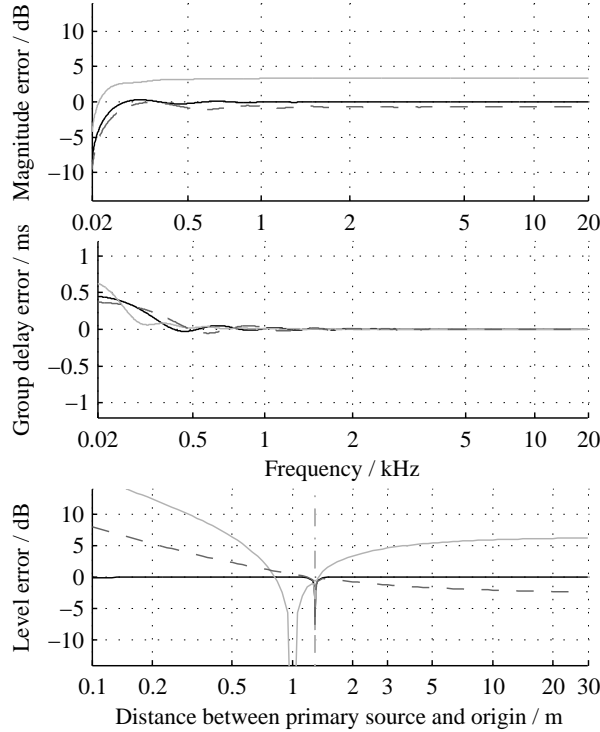
Fig. 7: Deviation from the targeted spherical field of the pressure field created by 2.5D WFS with a cylindrical primary field and the PSC introduced here using the large-argument approximations of the Hankel functions. Geometry identical to figure 1.

The data shown by figure 7 reveal the advantage of WFS with PSC even when using the Hankel functions' large-argument approximations: in contrast to earlier WFS derivations (cf. figures 4 and 5), the wave field is correct independently of the primary source position, except for primary sources directly at the secondary source contour.

Comparing equations 62 and 65, the numerical deviation between the driving functions for 2.5D WFS of spherical primary waves derived by Verheijen (1997) and given here is computed to

$$E_{2.5\mathrm{D,sw,ve}}(\mathbf{x}_0^{\mathrm{A}}, \mathbf{x}_{\mathrm{ref}}^{\mathrm{A}}, \mathbf{x}_{\mathrm{p}}^{\mathrm{A}}) \approx$$

$$\approx \frac{D_{2.5\mathrm{D,sw,ve}}(\mathbf{x}_0^{\mathrm{A}}|\mathbf{x}_{\mathrm{ref}}^{\mathrm{A}})}{D_{2.5\mathrm{D,sw}}(\mathbf{x}_0^{\mathrm{A}}|\mathbf{x}_{\mathrm{ref}}^{\mathrm{A}})} \qquad (66)$$

$$= \frac{1}{4\pi} \sqrt{\frac{\left|\mathbf{x}_{\mathrm{ref}}^{\mathrm{A}} - \mathbf{x}_{\mathrm{p}}^{\mathrm{A}}\right|}{\left|\mathbf{x}_0^{\mathrm{A}} - \mathbf{x}_{\mathrm{p}}^{\mathrm{A}}\right| + \left|\mathbf{x}_{\mathrm{ref}}^{\mathrm{A}} - \mathbf{x}_0^{\mathrm{A}}\right|}}.$$

Accordingly, equations 63 and 65 can be used to compute the deviation between the driving functions of Spors et al. (2008) and those derived here to

$$E_{2.5\mathrm{D,sw,sp}}(\mathbf{x}_0^{\mathrm{A}}, \mathbf{x}_{\mathrm{ref}}^{\mathrm{A}}, \mathbf{x}_{\mathrm{p}}^{\mathrm{A}}) \approx$$

$$\approx \frac{D_{2.5\mathrm{D,sw,sp}}(\mathbf{x}_0^{\mathrm{A}}|\mathbf{x}_{\mathrm{ref}}^{\mathrm{A}})}{D_{2.5\mathrm{D,sw}}(\mathbf{x}_0^{\mathrm{A}}|\mathbf{x}_{\mathrm{ref}}^{\mathrm{A}})} \qquad (67)$$

$$= \left(\frac{1}{\mathrm{j}k\left|\mathbf{x}_0^{\mathrm{A}} - \mathbf{x}_{\mathrm{p}}^{\mathrm{A}}\right|} + 1\right) \sqrt{\frac{\left|\mathbf{x}_{\mathrm{ref}}^{\mathrm{A}} - \mathbf{x}_{\mathrm{p}}^{\mathrm{A}}\right|}{\left|\mathbf{x}_0^{\mathrm{A}} - \mathbf{x}_{\mathrm{p}}^{\mathrm{A}}\right|}}.$$

Figure 8 shows at $f = 500\,\mathrm{Hz}$ the errors in magnitude for a primary point source at $\mathbf{x}_{\mathrm{p}}^{\mathrm{A}} = [2\ 0\ 0]^{\mathrm{T}}$ for the approaches given by equations 62, 63, and 65.
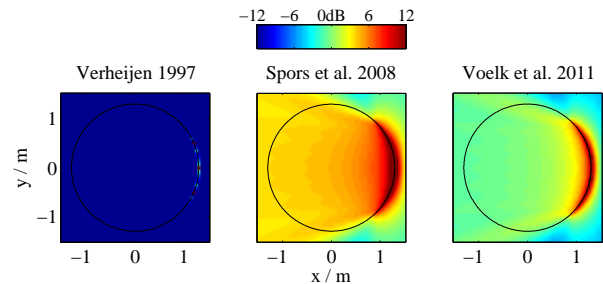
Fig. 8: Level deviation at $f = 500\,\mathrm{Hz}$ of the pressure field created by 2.5D wave field synthesis from the targeted field of a point source at $\mathbf{x}_{\mathrm{p}}^{\mathrm{A}} = [2\ 0\ 0]^{\mathrm{T}}$. Circular secondary source contour of 1.3 m radius (black).

This paper was presented at the 133$^{\mathrm{rd}}$ Convention of the Audio Engineering Society 2012, as paper number 8717.

Page 17 of 20

The circular secondary source contour of radius $1.3\,\mathrm{m}$ is indicated in black, the colors encode the position dependent level error of the 2.5D WFS in the range of $\pm 12\,\mathrm{dB}$.

The overall level error of the approach proposed by Verheijen (1997) is clearly visible in the left panel. Apart from this global shift, the errors for point sources are comparable to those resulting from the approach proposed here. However, focus points are represented more correctly by WFS with PSC as discussed here (cf. figures 4 and 7).

The error of the approach proposed by Spors et al. (2008) depends on the primary source position (cf. lower panel of figure 5), and also on the position within the secondary source contour, exceeding $6\,\mathrm{dB}$ in the case shown here (mid panel).

On the contrary, the approach proposed here by equation 65, shown by the right panel, allows despite the employment of the large-argument approximations of the Hankel functions a level error decaying to approximately zero at the reference point and in an extended section of the listening area. The level errors at positions farther from the secondary source contour than the reference point are on average negligible for many applications.

10. CONCLUSIONS

In this paper, the basic theory of wave field synthesis is revised for continuous secondary source contours, resulting in a global formulation of the secondary source correction that reduces the synthesis error over the whole listening area and allows for the correct reproduction of amplitude and phase at the reference point.

On that basis, the primary-source correction (PSC) for the 2D and 2.5D wave-field synthesis of spherical primary waves is discussed and extended to focus points. Wave-field synthesis with PSC permits at a reference point the correct synthesis of spherical waves respectively focus points evolving or located at arbitrary distances in the plane defined by the listening area. This especially includes the correct inverse proportionality of level and distance at the correct absolute level, which is shown not to result from earlier formulations of the 2D and 2.5D wave-field synthesis of primary point sources.

12. REFERENCES

Abramowitz M., I. A. Stegun: *Handbook of Mathematical Functions*. 10th Edition (United States of America, Department of Commerce, National Bureau of Standards, 1972) (Applied Mathematics Series 55)

Ahrens J., S. Spors: Implementation of Directional Sources in Wave Field Synthesis. In *IEEE Workshop on Applications of Signal Processing to Audio and Acoustics (WASPAA)* (2007)

Ahrens J., S. Spors: Notes on Rendering Focused Directional Virtual Sound Sources in Wave Field Synthesis. In *Fortschritte der Akustik, DAGA '08*, 229–230 (Dt. Gesell. für Akustik e. V., Berlin, 2008)

Baalman M. A. J.: Discretisation of complex sound sources for reproduction with Wave Field Synthesis. In *Fortschritte der Akustik, DAGA '05*, 209–210 (Dt. Gesell. für Akustik e. V., Berlin, 2005)

Baalman M. A. J.: Reproduction of arbitrarily shaped sound sources with Wave Field Synthesis – physical and perceptual effects. In *122nd AES Convention* (2007) (Convention Paper 7017)

Berkhout A. J.: A Holographic Approach to Acoustic Control. J. Audio Eng. Soc. **36**, 977–995 (1988)

Berkhout A. J., D. de Vries: Acoustic holography for sound control. In *86th AES Convention* (1989) (Preprint 2801)

Berkhout A. J., D. de Vries, P. Vogel: Acoustic control by wave field synthesis. J. Acoust. Soc. Am. **93**, 2764–2778 (1993)

Boone M. M., E. N. G. Verheijen, G. Jansen: Virtual Reality by Sound Reproduction Based on Wave Field Synthesis. In *100th AES Convention* (1996) (Preprint 4945)

Boone M. M., E. N. G. Verheijen, P. F. van Tol: Spatial Sound-Field Reproduction by Wave-Field Synthesis. J. Audio Eng. Soc. **43**, 1003–1012 (1995)

This paper was presented at the 133rd Convention of the Audio Engineering Society 2012, as paper number 8717.

Page 18 of 20

Bronstein I. N., K. A. Semendjajew, G. Musiol, H. Mühlig: *Taschenbuch der Mathematik (Handbook of mathematics)*. 5th Edition (Verlag Harri Deutsch, Frankfurt am Main, 2001)

Copley L. G.: Fundamental Results Concerning Integral Representations in Acoustic Radiation. J. Acoust. Soc. Am. **44**, 28–32 (1968)

Corteel E.: Synthesis of Directional Sources Using Wave Field Synthesis, Possibilities, and Limitations. EURASIP Journal on Advances in Signal Processing **2007**, Article ID 90509 (2007)

Corteel E.: On the use of irregularly spaced Loudspeaker Arrays for Wave Field Synthesis, Potential Impact on Spatial Aliasing Frequency. In *9th Int. Conference on Digital Audio Effects (DAFX '06)* (2006)

Corteel E., R. Pellegrini, C. Kuhn-Rahloff: Wave Field Synthesis with increased aliasing frequency. In *124th AES Convention* (2008) (Convention Paper 7362)

de Vries D.: Sound Reinforcement by Wavefield Synthesis: Adaptation of the Synthesis Operator to the Loudspeaker Directivity Characteristics. J. Audio Eng. Soc. **44**, 1120–1131 (1996)

Fastl H., E. Zwicker: *Psychoacoustics – Facts and Models*. 3rd Edition (Springer, Berlin, Heidelberg, 2007)

Fink M.: Time Reversal of Ultrasonic Fields – Part I: Basic Principles. IEEE Transactions on Ultrasonics, Ferroelectrics, and Frequency Control **39**, 555–566 (1992)

Fink M., C. Prada: Acoustic time-reversal mirrors. Inverse Problems **17**, R1–R38 (2001)

Gauthier P.-A., A. Berry: Adaptive wave field synthesis with independent radiation mode control for active sound field reproduction: Theory. J. Acoust. Soc. Am. **119**, 2721–2737 (2006)

Gauthier P.-A., A. Berry: Adaptive wave field synthesis for broadband active sound field reproduction: Signal processing. J. Acoust. Soc. Am. **123**, 2003–2016 (2008)

Jackson D. R., D. R. Dowling: Phase conjugation in underwater acoustics. J. Acoust. Soc. Am. **89**, 171–181 (1991)

Kim J. S., H. C. Song, W. A. Kuperman: Adaptive time-reversal mirror. J. Acoust. Soc. Am. **109**, 1817–1825 (2001)

Lucas B. G., T. G. Muir: The field of a focusing source. J. Acoust. Soc. Am. **72**, 1289–1296 (1982)

Marko H., ed. by J. Hagenauer: *Systemtheorie – Methoden und Anwendungen für ein- und mehrdimensionale Systeme (System Theory – Methods and Applications for one- and multidimensional Systems)*. 3rd Edition (Springer, Berlin, Heidelberg, New York, 1995)

Oppenheim A. V., A. S. Willsky, H. Nawab: *Signals and Systems*. 2nd Edition (Prentice-Hall, New Jersey, 1998)

Pierce A. D.: *Acoustics – An Introduction to its Physical Principles and Applications*. (Acoustical Society of America, Melville, NY, 1998)

Skudrzyk E.: *The Foundations of Acoustics - Basic Mathematics and Basic Acoustics*. (Springer, New York, Wien, 1971)

Sonke J.-J.: *Variable Acoustics by Wave Field Synthesis*, PhD thesis, Technische Universiteit Delft (2000)

Sonke J.-J., J. Labeeuw, D. de Vries: Variable Acoustics by Wavefield Synthesis: A Closer Look at Amplitude Effects. In *104th AES Convention* (1998) (Preprint 4712)

Spors S.: *Active Listening Room Compensation for Spatial Sound Reproduction Systems*, PhD thesis, Friedrich-Alexander-Universität Erlangen-Nürnberg (2005)

Spors S.: An Analytic Secondary Source Selection Criterion for Wavefield Synthesis. In *Fortschritte der Akustik, DAGA 2007*, 679–680 (Dt. Gesell. für Akustik e. V., Berlin, 2007a)

Spors S.: Extension of an Analytic Secondary Source Selection Criterion for Wave Field Synthesis. In *123rd AES Convention* (2007b) (Convention Paper 7299)

This paper was presented at the 133rd Convention of the Audio Engineering Society 2012, as paper number 8717.

Page 19 of 20

Spors S., J. Ahrens: Spatial Sampling Artifacts of Wave Field Synthesis for the Reproduction of Virtual Point Sources. In *126th AES Convention* (2009) (Convention Paper 7744)

Spors S., J. Ahrens: Analysis and Improvement of Pre-equalization in 2.5-Dimensional Wave Field Synthesis. In *128th AES Convention* (2010) (Convention Paper 8121)

Spors S., R. Rabenstein, J. Ahrens: The Theory of Wave Field Synthesis Revisited. In *124th AES Convention* (2008) (Convention Paper 7358)

Start E. W.: Application of Curved Arrays in Wave Field Synthesis. In *100th AES Convention* (1996) (Preprint 4143)

Start E. W.: *Direct sound enhancement by wave field synthesis*, PhD thesis, Technische Universiteit Delft (1997)

Start E. W., M. S. Roovers, D. de Vries: In Situ Measurement on a Wave Field Synthesis System For Sound Enhancement. In *102nd AES Convention* (1997) (Preprint 4454)

Tanter M., J.-F. Aubry, J. Gerber, J.-L. Thomas, M. Fink: Optimal focusing by spatio-temporal inverse filter. I. Basic principles. J. Acoust. Soc. Am. **110**, 37–47 (2001)

Verheijen E. N. G.: *Sound Reproduction by Wave Field Synthesis*, PhD thesis, Technische Universiteit Delft (1997)

Vogel P.: *Application of Wave Field Synthesis in Room Acoustics*, PhD thesis, Technische Universiteit Delft (1993)

Völk F.: Psychoakustische Experimente zur Distanz mittels Wellenfeldsynthese erzeugter Hörereignisse (Psychoacoustic experiments on the distance of auditory events in wave field synthesis). In *Fortschritte der Akustik, DAGA 2010*, 1065–1066 (Dt. Gesell. für Akustik e. V., Berlin, 2010)

Völk F., F. Lindner, H. Fastl: Primary Source Correction (PSC) in Wave Field Synthesis. In *ICSA 2011 – International Conference on Spatial Audio* (Verband deutscher Tonmeister, VDT, 2011)

Völk F., U. Mühlbauer, H. Fastl: Minimum Audible Distance (MAD) by the Example of Wave Field Synthesis. In *Fortschritte der Akustik, DAGA 2012*, 319–320 (Dt. Gesell. für Akustik e. V., Berlin, 2012)

Vorländer M.: *Auralization – Fundamentals of Acoustics, Modelling, Simulation, Algorithms and Acoustic Virtual Reality.* (Springer, Berlin, Heidelberg, 2008)

Warufsel O., E. Corteel, N. Misdariis, T. Caulkins: Reproduction of sound source directivity for future audio applications. In *18th Int. Congress on Acoustics (ICA)* (2004)

Williams E. G.: *Fourier Acoustics – Sound Radiation and Nearfield Acoustical Holography.* (Academic Press, San Diego, London, 1999)

Wittek H., F. Rumsey, G. Theile: Perceptual Enhancement of Wavefield Synthesis by Stereophonic Means. J. Audio Eng. Soc. **55**, 723–751 (2007)

Wittek H., S. Kerber, F. Rumsey, G. Theile: Spatial perception in Wave Field Synthesis rendered sound fields: Distance of real and virtual nearby sources. In *116th AES Convention* (2004) (Convention Paper 6000)

Yon S., M. Tanter, M. Fink: Sound Focusing in rooms. II. The spatio-temporal inverse filter. J. Acoust. Soc. Am. **114**, 3044–3052 (2003a)

Yon S., M. Tanter, M. Fink: Sound focusing in rooms: The time-reversal approach. J. Acoust. Soc. Am. **113**, 1533–1543 (2003b)

Zahorik P.: Assessing auditory distance perception using virtual acoustics. J. Acoust. Soc. Am. **111**, 1832–1846 (2002)

Zahorik P., D. S. Brungart, A. W. Bronkhorst: Auditory Distance Perception in Humans: A Summary of Past and Present Research. Acta Acustica united with Acustica **91**, 409–420 (2005)

Zollner M., E. Zwicker: *Elektroakustik (Electroacoustics).* 3rd Edition (Springer, Berlin, 1993)

This paper was presented at the 133rd Convention of the Audio Engineering Society 2012, as paper number 8717.

Page 20 of 20